

Privacy-Preserving Verifiable Neural Network Inference Service

Arman Riasi
Virginia Tech
armanriasi@vt.edu

Jorge Guajardo
Robert Bosch LLC — RTC
jorge.guajardomerchan@us.bosch.com

Thang Hoang
Virginia Tech
thanghoang@vt.edu

Abstract—Machine learning has revolutionized data analysis and pattern recognition, but its resource-intensive training has limited accessibility. Machine Learning as a Service (MLaaS) simplifies this by enabling users to delegate their data samples to an MLaaS provider and obtain the inference result using a pre-trained model. Despite its convenience, leveraging MLaaS poses significant privacy and reliability concerns to the client. Specifically, sensitive information from the client inquiry data can be leaked to an adversarial MLaaS provider. Meanwhile, the lack of a verifiability guarantee can potentially result in biased inference results or even unfair payment issues. While existing trustworthy machine learning techniques, such as those relying on verifiable computation or secure computation, offer solutions to privacy and reliability concerns, they fall short of simultaneously protecting the privacy of client data and providing provable inference verifiability.

In this paper, we propose vPIN, a privacy-preserving and verifiable CNN inference scheme that preserves privacy for client data samples while ensuring verifiability for the inference. vPIN makes use of partial homomorphic encryption and commit-and-prove succinct non-interactive argument of knowledge techniques to achieve desirable security properties. In vPIN, we develop various optimization techniques to minimize the proving circuit for homomorphic inference evaluation thereby, improving the efficiency and performance of our technique. We fully implemented and evaluated our vPIN scheme on standard datasets (e.g., MNIST, CIFAR-10). Our experimental results show that vPIN achieves high efficiency in terms of proving time, verification time, and proof size, while providing client data privacy guarantees and provable verifiability.

Index Terms—privacy-preserving, verifiable neural network inference

I. INTRODUCTION

Machine learning (ML) has revolutionized the way computers interact with data, allowing them to acquire knowledge from data on their own, without the limitations of explicit programming. Deep learning, especially Convolutional Neural Networks (CNNs), has revolutionized the field of visual data analysis, enabling applications such as image classification and object recognition. However, addressing the extensive data demands of model training, computational resource constraints, and implementation expertise has led to the rise of Machine Learning as a Service (MLaaS). MLaaS is a cloud-based platform that provides access to powerful ML-assisted services (e.g., analysis, inference, prediction). Typically, MLaaS providers such as Microsoft Azure [1], Google Cloud AI Platform [2], Amazon AWS [3], Face++ [4], and Clarifai [5]

operate on a pay-as-you-go model, where clients pay based on their resource usage for inference.

Despite its benefits, delegating ML tasks to a server raises some privacy concerns. An adversarial server can misuse the private information of the client data. Additionally, the lack of a mechanism to verify ML operations performed by the server introduces integrity and trustworthiness issues. This becomes essential since an adversarial server may process the client request arbitrarily without relying on a dependable ML model. Moreover, there is a risk of unfair payment, where the server may charge the client more than its actual resource consumption. Consequently, the outcome of the delegated ML processing tasks can be untrustworthy.

To address the aforementioned privacy and trustworthiness issues in ML, several research directions have been suggested. One line of research focuses on verifiable Machine Learning (verifiable ML), which aims to ensure the verifiability of ML computations and address concerns regarding unfair payment by requiring the server to provide mathematical proof of correct computations. Some studies, such as Safetynets [6] and VeriML [7], investigate Verifiable Computation techniques (e.g., [8], [9]) that enable the client to effectively verify the correctness of computations performed by an MLaaS server. Moreover, some verifiable ML research incorporates zero knowledge property into proofs (e.g., [10], [11], [12], [13], [14], [15], [16]) to improve server model privacy. While these studies effectively address computation integrity and overcharging concerns, the main limitation of existing verifiable ML schemes is that they do not offer privacy to the client data, where the client has to send their sample (in plaintext) to the server for inference service.

The other research line focuses on Privacy-Preserving ML (PPML), in which secure computation techniques such as Homomorphic Encryption (HE) [17] and/or Multi-party Computation (MPC) [18] have been used, to protect the privacy of both client data and server model parameters during the ML evaluation. However, these techniques may not be suitable for MLaaS applications. Specifically, HE-based PPML approaches [19], [20], [21], [22], [23] do not offer computation verifiability. Consequently, the server can employ low-quality model parameters to process computation on encrypted client data, thereby making results unreliable. Meanwhile, MPC-based approaches [24], [25], [26], [27] require distributed systems with multiple non-colluding computationally resourceful entities, which may

significantly increase the deployment and operational costs.

While existing research attempts to address privacy and verifiability concerns in ML inference schemes, a critical gap persists in ensuring client data privacy within verifiable ML schemes. Therefore, we raise the following question:

Can we design a new privacy-preserving and verifiable ML inference scheme that not only preserves the privacy of the client data but also guarantees computational and provable verifiability with efficient performance?

Our Contributions. In this paper, we introduce vPIN, a new privacy-preserving and verifiable ML inference scheme that allows the client to use remote ML inference services with data privacy and inference result integrity guarantees. vPIN focuses on the standard CNN inference framework with multiple processing layers such as convolution, activation, pooling, and fully connected layers. vPIN relies on two core building blocks including partial homomorphic encryption and commit-and-prove Succinct Non-interactive Argument of Knowledge (SNARK) to enable client privacy and server computation integrity, respectively. We provide detailed gadgets to represent arithmetic constraints for ciphertext operations (§IV-A). These gadgets are not only critical for proving CNN inference evaluation on the encrypted data but also can be found useful in other applications. vPIN addresses the challenges of proving complicated ML functions on the encrypted domains by incorporating new techniques to reduce the circuit complexity including elliptic curve embedding and probabilistic matrix multiplication check. As a result, vPIN achieves markedly higher efficiency compared to the baseline approaches that hardcode the whole CNN inference computation on the encrypted data into the proving circuit.

We provide a formal security definition for privacy-preserving and verifiable ML inference with client data privacy and verifiability, and prove that vPIN satisfies all the security properties. We fully implemented and evaluated our vPIN scheme, assessing its performance on real dataset and comparing it with the baseline setting in terms of proving time, verification time, and proof size. The source code for our implementation can be found at

<https://github.com/vt-asaplab/vPIN>

Remark. In this work, we only focus on user privacy and verifiability in place of server privacy. It is a challenging task to enable privacy for both the user and server simultaneously. Adding the zero-knowledge property to SNARK can only protect the server’s model privacy in the proof; however, the model can still be leaked from the plain inference outputs (e.g., via model extraction/stealing attacks [28], [29], [30], [31], [32]). Therefore, we defer the investigation that can fully protect the server model privacy as our future work.

Applications Scenarios. Our proposed scheme can be useful in some applications in medical diagnosis and financial forecasting [33], [34], [35], [36]. For instance, in medical diagnosis, healthcare providers might use MLaaS inference to analyze private client medical data, such as lung images, for infection detection. However, incorrect model predictions could have

a serious impact, especially if the cloud provider fails to use the actual model. Additionally, outsourcing client medical data could potentially pose some complications. To address them, vPIN allows healthcare providers to encrypt the image before sharing them with the MLaaS provider. Moreover, using our scheme, the healthcare provider can verify that the correct model is used to process the image and ensure charge accuracy based on resource usage, thus preventing overbilling.

In financial forecasting, businesses may use MLaaS inference to analyze datasets and make decisions about investments, market trends, and risk management. Like medical diagnosis, these datasets contain sensitive business information that cannot be shared with an MLaaS provider. Furthermore, ensuring the correct model parameters are used for prediction in financial forecasting is crucial, as it can have real-world implications (e.g., financial losses, missed opportunities). Therefore, vPIN can address these concerns by processing financial data in encrypted form and providing inference verifiability to ensure the correct model is employed.

II. PRELIMINARIES

Notation. Let $\mathbb{Z}_n = \{0, 1, 2, \dots, n\}$ and $\mathbb{Z}_n^* = \mathbb{Z}_n \setminus \{0\}$. λ denotes security parameters, and $\text{negl}(\cdot)$ stands for the negligible function. $x \xleftarrow{\$} \mathbb{Z}_n$ indicates that x is chosen randomly from the set \mathbb{Z}_n . PPT refers to Probabilistic Polynomial Time. $A \stackrel{c}{\approx} B$ indicates computational indistinguishability of two quantities A and B . Bold letters (like \mathbf{a} and \mathbf{A}) denote vector and matrix, respectively. $\mathbf{a}[i]$ represents the element i in vector \mathbf{a} . $\mathbf{A}[i, j]$ refers to the element at row i and column j in matrix \mathbf{A} . \mathbf{A}^T denotes the transpose of \mathbf{A} . \mathbb{G} represents the cyclic group in which $\llbracket 1 \rrbracket \in \mathbb{G}$ denotes a random generator of \mathbb{G} . The group element $\llbracket x \rrbracket$ in \mathbb{G} has a discrete logarithm of x with base $\llbracket 1 \rrbracket$, where $x \in \mathbb{Z}_q$ (q is the order of \mathbb{G}). Group operations are additive, thus $\llbracket x \rrbracket + \llbracket y \rrbracket$ equals $\llbracket x + y \rrbracket \in \mathbb{G}$ and scalar multiplication over group \mathbb{G} is represented as $\delta \cdot \llbracket x \rrbracket \in \mathbb{G}$, where scalar $\delta \in \mathbb{Z}_q$. We denote the convolution operation between two matrices as $\mathbf{C} = \mathbf{A} * \mathbf{B}$ where $\mathbf{C}[i, j] = \sum_{i'=0}^{k-1} \sum_{j'=0}^{k-1} \mathbf{A}[i \cdot \hat{s} + i', j \cdot \hat{s} + j'] \cdot \mathbf{B}[i', j']$, \mathbf{B} is a $k \times k$ matrix, and \hat{s} is the stride size.

A. Additive Homomorphic Encryption

Additive Homomorphic Encryption (AHE) [37] is a public-key encryption that permits plaintext messages to be encrypted in a way that their ciphertexts can be homomorphically evaluated. An AHE scheme consists of the following algorithms.

- $(\text{pk}, \text{sk}) \leftarrow \text{AHE.KeyGen}(1^\lambda)$: Given a security parameter λ , it outputs a pair of public key and private key (pk, sk) .
- $c \leftarrow \text{AHE.Enc}(\text{pk}, m)$: Given a message m and a public key pk , it outputs a ciphertext c .
- $m \leftarrow \text{AHE.Dec}(\text{sk}, c)$: Given a ciphertext c and a private key sk , it outputs a plaintext message m .

Homomorphism. Let $m_1 \in \mathbb{Z}_n$, $m_2 \in \mathbb{Z}_n$ be plaintext messages, AHE offers additive homomorphic properties as

- Ciphertext addition: Let \boxplus be the group addition over the AHE ciphertext domain. We have that $\text{AHE.Dec}(\text{sk}, \text{AHE.Enc}(\text{pk}, m_1) \boxplus \text{AHE.Enc}(\text{pk}, m_2)) = (m_1 + m_2)$

- **Scalar multiplication:** Let \boxtimes be the group scalar multiplication over the AHE ciphertext domain. We have that
$$\text{AHE.Dec}(\text{sk}, m_2 \boxtimes \text{AHE.Enc}(\text{pk}, m_1)) = m_1 \cdot m_2$$

We present the correctness and IND-CPA security of the AHE scheme in Appendix §A.

B. Commit-and-Prove Argument Systems

Commit-and-Prove SNARK (CP-SNARK) [10] permits a prover to commit to a witness w in advance for an NP-statement $(\mathcal{R}, \mathcal{L})$, where \mathcal{R} is an NP relation and \mathcal{L} is the language of valid inputs. Given $x \in \mathcal{L}$, the prover proves the knowledge of w that satisfies the NP relation \mathcal{R} , i.e., $(x, w) \in \mathcal{R}$. CP-SNARK is a tuple of PPT algorithms $\text{CPS} = (\text{Setup}, \text{Comm}, \text{Prov}, \text{Ver})$ as follows.

- $\text{pp} \leftarrow \text{CPS.Setup}(1^\lambda)$: Given a security parameter λ , it outputs public parameters pp .
- $\text{cm} \leftarrow \text{CPS.Comm}(w, r, \text{pp})$: Given a witness w and randomness r , it outputs cm as a commitment to w .
- $\pi \leftarrow \text{CPS.Prov}(x, w, \text{pp})$: Given a statement x and a witness w , it outputs a proof π that shows $(x, w) \in \mathcal{R}$.
- $b \leftarrow \text{CPS.Ver}(\pi, \text{cm}, x, \text{pp})$: Given a proof π , a commitment cm , and a statement x , it outputs b where b is 1 (accept) if π is a valid proof for $(x, w) \in \mathcal{R}$ and cm is a commitment to w ; otherwise, it outputs 0 (reject).

Definition 1. CP-SNARK satisfies the following security properties.

- **Completeness:** For any $\lambda, r, (x, w) \in \mathcal{R}$ s.t. $\text{pp} \leftarrow \text{CPS.Setup}(1^\lambda)$, $\text{cm} \leftarrow \text{CPS.Comm}(w, r, \text{pp})$, and $\pi \leftarrow \text{CPS.Prov}(x, w, \text{pp})$,

$$\Pr[\text{CPS.Ver}(\pi, \text{cm}, x, \text{pp}) = 1] = 1$$

- **Knowledge soundness:** For any PPT \mathcal{P}^* , and statement x , there exists a PPT extractor \mathcal{E} that, with access to the entire execution process and the randomness of \mathcal{P}^* , can extract a witness w s.t. $\text{pp} \leftarrow \text{CPS.Setup}(1^\lambda)$, $\text{cm} \leftarrow \text{CPS.Comm}(w, r, \text{pp})$ for randomness r , $\pi^* \leftarrow \mathcal{P}^*(x, \text{pp})$, $w \leftarrow \mathcal{E}^{\mathcal{P}^*}(x, \pi^*, \text{pp})$, it holds that
$$\Pr[(x, w) \notin \mathcal{R} \wedge \text{CPS.Ver}(\pi^*, \text{cm}, x, \text{pp}) = 1] \leq \text{negl}(\lambda)$$

C. Convolutional Neural Networks

CNNs [38], [39] allow learning hierarchical features from data for tasks such as image classification and recognition. CNNs consist of multiple consecutive layers as follows.

Convolutional Layer. It extracts features from data samples by computing dot products between overlapping sections of an $n \times m$ input samples \mathbf{X} and a $k \times k$ filter \mathbf{K} as $\mathbf{A} = \mathbf{X} * \mathbf{K}$ (2D convolution).

Activation Layer. It introduces non-linearity by applying non-linear functions on the $n' \times m'$ convolution output to enable the network to learn complex and non-linear patterns in the data. In this paper, we focus on ReLU as the activation function, which is defined as $\mathbf{B}[i, j] = \max(0, \mathbf{A}[i, j])$ for $i \in [0, n']$, $j \in [0, m']$.

Pooling Layer. It reduces the spatial dimensions of the $n' \times m'$ activation layer output by applying functions such as average

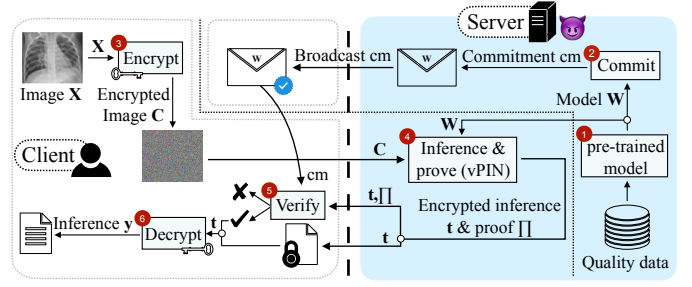


Fig. 1: The overall architectural model of vPIN.

pooling or max pooling. In this paper, we use the average pooling such that $\mathbf{C}[i, j] = \frac{1}{k^2} \sum_{i'=0}^{k-1} \sum_{j'=0}^{k-1} \mathbf{B}[i \cdot \hat{k} + i', j \cdot \hat{k} + j']$ with $\hat{k} \times \hat{k}$ window.

Fully Connected (FC) Layer. It combines high-level features extracted from earlier layers to establish the complex relationships between the different features. We define the FC layer as $\mathbf{e}[i] = (\sum_{j=0}^g \mathbf{W}^T[i, j] \cdot \mathbf{d}[j]) + \mathbf{b}[i]$ for $i \in [0, h]$, where g, h denote the FC layer input and output sizes, respectively, \mathbf{W} is the model weight parameters, \mathbf{d} is the $\hat{n} \times \hat{m}$ pooling layer output flattened such that $\mathbf{d}[i \cdot \hat{n} + j] = \mathbf{C}[i, j]$ for $i \in [0, \hat{n}]$, $j \in [0, \hat{m}]$, and \mathbf{b} is the bias vector.

III. MODEL

System Model. Our vPIN system consists of two parties: the server and the client. The server holds well-trained ML model parameters $\mathbf{W} \in \mathcal{M}_{\text{pp}}$ where \mathcal{M}_{pp} denotes model space. The client holds a private data sample $\mathbf{X} \in \mathcal{N}_{\text{pp}}$, where \mathcal{N}_{pp} denotes message space. The server commits to the ML model \mathbf{W} and allows a client to perform inference on her data sample \mathbf{X} using its committed model while preserving the privacy of the data sample, and guaranteeing computational correctness. Figure 1 illustrates system workflow of vPIN. Initially, we assume that the server owns an ML model pre-trained from a high-quality data source (1). The server commits to this model beforehand (2). In vPIN, the client encrypts her data sample and sends it to the server (3). The server then performs the inference on the encrypted data and generates a proof of correct inference computations based on the committed model (4). Finally, the client verifies the proof (5) and decrypts to obtain the inference result (6). Formally speaking, our vPIN is a privacy-preserving and verifiable ML inference scheme as $\text{vPIN} = (\text{Setup}, \text{Comm}, \text{Enc}, \text{Infer}, \text{Dec})$ as follows.

- $(\text{sk}, \text{pk}, \text{pp}) \leftarrow \text{vPIN.Setup}(1^\lambda, l)$: Given a security parameter λ and an upper bound of the size of model parameter l , it outputs a pair of public-private key (pk, sk) and public parameters pp .
- $\text{cm} \leftarrow \text{vPIN.Comm}(\mathbf{W}, r, \text{pp})$: Given ML model parameters $\mathbf{W} \in \mathcal{M}_{\text{pp}}$ and a randomness $r \in \mathcal{R}_{\text{pp}}$ where \mathcal{R}_{pp} is the random space, it outputs a commitment $\text{cm} \in \mathcal{D}_{\text{pp}}$, where \mathcal{D}_{pp} is the commitment space.
- $\mathbf{C} \leftarrow \text{vPIN.Enc}(\text{pk}, \mathbf{X}, \text{pp})$: Given a public key pk and a data sample $\mathbf{X} \in \mathcal{N}_{\text{pp}}$, it outputs a ciphertext $\mathbf{C} \in \mathcal{C}_{\text{pp}}$, where \mathcal{C}_{pp} denotes ciphertext space.

- $(\pi, \mathbf{t}) \leftarrow \text{vPIN.Infer}(\mathbf{W}, \mathbf{C}, \text{pp})$: Given ML model parameters $\mathbf{W} \in \mathcal{M}_{\text{pp}}$ and an encrypted data sample $\mathbf{C} \in \mathcal{C}_{\text{pp}}$, it outputs an encrypted inference result $\mathbf{t} = \mathcal{F}(\mathbf{W}, \mathbf{C}) \in \mathcal{C}_{\text{pp}}$ (where \mathcal{F} is the ideal ML inference functionality) and a proof π .
- $\{\mathbf{y}, \perp\} \leftarrow \text{vPIN.Dec}(\text{sk}, \mathbf{t}, \text{cm}, \pi, \text{pp})$: Given a private key sk , an encrypted inference $\mathbf{t} \in \mathcal{C}_{\text{pp}}$, a commitment $\text{cm} \in \mathcal{D}_{\text{pp}}$, and a proof π , it outputs a plaintext inference $\mathbf{y} \in \mathcal{N}_{\text{pp}}$ if π is a valid proof for the inference computation; otherwise it outputs \perp .

Threat Model. In our system, we assume the client to be honest. The server can behave maliciously to compromise client data and the integrity of the inference computation by employing arbitrary model parameters or an arbitrary data sample instead of the actual ones. In this paper, we aim to preserve the privacy of the client data sample against the server while ensuring the integrity of the inference computation.

Security Model. We define the security definition of our privacy-preserving and verifiable ML inference, which guarantees the privacy of data samples and the integrity of inferences as follows.

Definition 2. A privacy-preserving and verifiable ML satisfies the following security properties.

- **Completeness.** For any $\lambda, l, \mathbf{W} \in \mathcal{M}_{\text{pp}}, \mathbf{X} \in \mathcal{N}_{\text{pp}}, r \in \mathcal{R}_{\text{pp}}$ s.t. $(\text{sk}, \text{pk}, \text{pp}) \leftarrow \text{vPIN.Setup}(1^\lambda, l)$, $\text{cm} \leftarrow \text{vPIN.Comm}(\mathbf{W}, r, \text{pp})$, $\mathbf{C} \leftarrow \text{vPIN.Enc}(\text{pk}, \mathbf{X}, \text{pp})$, $(\pi, \mathbf{t}) \leftarrow \text{vPIN.Infer}(\mathbf{W}, \mathbf{C}, \text{pp})$,

$$\Pr[\text{vPIN.Dec}(\text{sk}, \mathbf{t}, \text{cm}, \pi, \text{pp}) \neq \perp] = 1$$

- **Soundness.** For any λ, l , and PPT adversary \mathcal{A} , it holds that

$$\Pr \left[\begin{array}{l} (\text{sk}, \text{pk}, \text{pp}) \leftarrow \text{vPIN.Setup}(1^\lambda, l) \\ (\text{cm}^*, \mathbf{W}^*, \mathbf{C}, \mathbf{t}^*, \pi^*, r) \leftarrow \mathcal{A}(\text{pk}, \text{pp}) \\ \text{cm}^* = \text{vPIN.Comm}(\mathbf{W}^*, r, \text{pp}) \\ \text{vPIN.Dec}(\text{sk}, \mathbf{t}^*, \text{cm}^*, \pi^*, \text{pp}) \neq \perp \\ \mathcal{F}(\mathbf{W}^*, \mathbf{C}) \neq \mathbf{t}^* \end{array} \right] \leq \text{negl}(\lambda)$$

- **Data sample and inference privacy.** For any $\lambda, l, \mathbf{X} \in \mathcal{N}_{\text{pp}}$ such that $(\text{sk}, \text{pk}, \text{pp}) \leftarrow \text{vPIN.Setup}(1^\lambda, l)$, and PPT adversary \mathcal{A} , there exists a simulator \mathcal{S}' such that

$$\Pr \left[\mathcal{A}(\text{pk}, \mathbf{C}, \mathbf{t}, \text{pp}) = 1 \mid \begin{array}{l} \mathbf{C} \leftarrow \text{vPIN.Enc}(\text{pk}, \mathbf{X}, \text{pp}) \\ (\pi, \mathbf{t}) \leftarrow \text{vPIN.Infer}(\mathbf{W}, \mathbf{C}, \text{pp}) \end{array} \right] \\ \approx \Pr \left[\mathcal{A}(\text{pk}, \mathbf{C}, \mathbf{t}, \text{pp}) = 1 \mid (\mathbf{t}, \mathbf{C}) \leftarrow \mathcal{S}'(\text{pk}, |\mathbf{X}|, \text{pp}) \right]$$

Out-of-Scope Attacks. In this paper, we assume the client to be honest and, therefore, do not consider model extraction/stealing attacks [28], [29], [30], [31], [32] that aim to compromise the server model privacy by collecting query-response pairs from the target model. For dishonest clients, several countermeasures can be considered such as model extraction detection [40], [31], [41], [42], [43], limited queries [42], query pattern recognition [31], [41], and differential privacy [44], [45]. We leave the investigation of how to apply these techniques under encryption as our future work.

IV. OUR PROPOSED METHOD

vPIN employs an AHE scheme based on an Elliptic Curve (EC) to encrypt user data. To prove the correctness of inference

over encrypted data, we need to provide arithmetic constraints. We first introduce necessary gadgets in vPIN, which are intermediate arithmetic constraint systems for computation statements. We then present our vPIN construction in detail.

A. Building Block Gadgets

We introduce arithmetic constraints that are required for EC point addition and point multiplication.

Reverse Binarization Gadget. We present a reverse binarization gadget based on the binarization gadget [16]. Given a value $a \in \mathbb{Z}_k$ and a vector $\mathbf{v} \in \mathbb{Z}_2^n$, the reverse binarization gadget $\text{RevBin}(a, \mathbf{v}, n)$ can generate the arithmetic constraints to demonstrate that \mathbf{v} is a reverse binary representation of a as follows:

$$\begin{cases} \mathbf{v}[i] \times \mathbf{v}[i] = \mathbf{v}[i] \text{ for } i \in [1, n] \\ \sum_{i=1}^n \mathbf{v}[n-i] \cdot 2^{n-i-1} = a \end{cases} \quad (1)$$

EC Point Addition Gadget. Given three EC points $A = (x_a, y_a) \in \mathbb{Z}_p^2$, $B = (x_b, y_b) \in \mathbb{Z}_p^2$, and $C = (x_c, y_c) \in \mathbb{Z}_p^2$ on curve $E : y^2 = x^3 + \alpha x + \beta$ where $\alpha, \beta \in \mathbb{Z}_p$, we present a point addition gadget $\text{PtAdd}(C, A, B)$ to demonstrate the arithmetic constraints for $C = A + B$. Let $\text{aux}_1, \text{aux}_2, \text{aux}_3$, and $\text{aux}_4 \in \mathbb{Z}_p$ be auxiliary witnesses. The set of arithmetic constraints for an ECC point addition is

$$\begin{cases} \text{aux}_1 = (x_b - x_a)^{-1} \pmod p \\ \text{aux}_2 = (y_b - y_a) \cdot \text{aux}_1 \pmod p \\ \text{aux}_3 = \text{aux}_2 \cdot \text{aux}_2 \pmod p \\ x_c = \text{aux}_3 - x_a - x_b \pmod p \\ \text{aux}_4 = \text{aux}_2 \cdot (x_a - x_c) \pmod p \\ y_c = \text{aux}_4 - y_a \pmod p \end{cases} \quad (2)$$

EC Point Doubling Gadget. Given two EC points $A = (x_a, y_a) \in \mathbb{Z}_p^2$ and $D = (x_d, y_d) \in \mathbb{Z}_p^2$ on curve $E : y^2 = x^3 + \alpha x + \beta$ where $\alpha, \beta \in \mathbb{Z}_p$, we present a point doubling gadget $\text{PtDb}(D, A)$ that demonstrates the arithmetic constraints for $D = 2A$. Let $\text{aux}_1, \text{aux}_2, \text{aux}_3, \text{aux}_4$, and $\text{aux}_5 \in \mathbb{Z}_p$ be auxiliary witnesses. The set of arithmetic constraints for an ECC point doubling is

$$\begin{cases} \text{aux}_1 = (2y_a)^{-1} \pmod p \\ \text{aux}_2 = x_a \cdot x_a \pmod p \\ \text{aux}_3 = (3\text{aux}_2 + \alpha) \cdot \text{aux}_1 \pmod p \\ \text{aux}_4 = \text{aux}_3 \cdot \text{aux}_3 \pmod p \\ x_d = \text{aux}_4 - 2x_a \pmod p \\ \text{aux}_5 = \text{aux}_3 \cdot (x_a - x_d) \pmod p \\ y_d = \text{aux}_5 - y_a \pmod p \end{cases} \quad (3)$$

Point Multiplication Gadget. Given a scalar $w \in \mathbb{Z}_p$, two EC points $Q = (x_q, y_q) \in \mathbb{Z}_p^2$ and $P = (x_p, y_p) \in \mathbb{Z}_p^2$ on curve $E : y^2 = x^3 + \alpha x + \beta$ where $\alpha, \beta \in \mathbb{Z}_p$, we present point multiplication gadget $\text{PtMul}(Q, w, P)$ that demonstrates the arithmetic constraints for $Q = w \cdot P$. Since we use the index-increasing approach of the *double-and-add* algorithm, we employ the RevBin gadget to represent the scalar multiplier

w as a binary number in the reversed order, with the least significant bit (LSB) at index 0 and the most significant bit (MSB) at the last index of \mathbf{v} . Along with RevBin, we also employ PtAdd and PtDbl gadgets to enable iterative point addition and doubling in the *double-and-add* algorithm. In that case, the arithmetic constraints are as follows:

$$\begin{cases} \text{RevBin}(w, \mathbf{v}, n) \\ A_0 = P \\ B_0 = \infty^1 \\ \text{PtAdd}(C_i, B_{i-1}, A_{i-1}) \text{ for } i \in [1, n] \\ \text{PtDbl}(D_i, A_{i-1}) \text{ for } i \in [1, n] \\ B_i = (\mathbf{v}[i] \cdot C_i) + ((1 - \mathbf{v}[i]) \cdot C_{i-1}) \pmod p \text{ for } i \in [1, n] \\ A_i = D_i \text{ for } i \in [1, n] \\ Q = B_n \end{cases} \quad (4)$$

B. Detailed vPIN Construction

We are now ready to present vPIN in detail, including its setup, commitment, encryption, inference, and decryption algorithms. Due to space constraints, we present the pseudocode of these algorithms in Appendix §B.

1) *Setup procedure*: This procedure generates the necessary parameters to ensure the privacy of the client’s data sample and the verifiability of inference computations. These include public parameters pp for the underlying CP-SNARK and a public-private key pair (sk, pk) for the back-end AHE scheme. To do so, we first identify suitable cyclic groups (i.e., EC parameters) used in CP-SNARK and AHE. Note that in vPIN, the server performs homomorphic evaluations between its model parameter and the (encrypted) client’s sample and creates a proof of correct homomorphic evaluation. That means the proof circuit for such homomorphic evaluations can be extremely large if the parameters are not selected properly.

For instance, let curve E_1 be the cyclic group of CP-SNARK with base field \mathbb{Z}_{n_1} and order q_1 , and curve E_2 be the cyclic group of AHE with base field \mathbb{Z}_{n_2} and order q_2 . Let $w \in \mathbb{Z}_{q_2}$ be the (plaintext) server model, and $\llbracket C \rrbracket_2 = (x_c, y_c) \in \mathbb{Z}_{n_2}^2$ be the AHE-encrypted client data sample. Suppose $w = 2$ for simplicity, the set of arithmetic constraints under CP-SNARK based on (3) for the homomorphic evaluation of $\llbracket w \cdot C \rrbracket_2$ is as follows:

$$\begin{cases} \text{aux}_1 = ((2y_c)^{-1} \pmod{n_2}) \pmod{q_1} \\ \text{aux}_2 = (x_c \cdot x_c \pmod{n_2}) \pmod{q_1} \\ \text{aux}_3 = ((3\text{aux}_2 + \alpha) \cdot \text{aux}_1 \pmod{n_2}) \pmod{q_1} \\ \text{aux}_4 = (\text{aux}_3 \cdot \text{aux}_3 \pmod{n_2}) \pmod{q_1} \\ x_d = (\text{aux}_4 - 2x_c \pmod{n_2}) \pmod{q_1} \\ \text{aux}_5 = (\text{aux}_3 \cdot (x_c - x_d) \pmod{n_2}) \pmod{q_1} \\ y_d = (\text{aux}_5 - y_c \pmod{n_2}) \pmod{q_1} \end{cases} \quad (5)$$

We can see that each arithmetic constraint in (5) requires creating costly modular arithmetic circuits for proving modulo n_2 . For instance, to prove the relation $\hat{\text{aux}} = \hat{x} \cdot \hat{y} \pmod{n_2}$

¹This can be achieved using an indicator for the point at infinity.

where $\hat{x}, \hat{y} \in \mathbb{Z}_{n_2}$, we require 23 constraints according to the most efficient modular multiplication gadget in [46]. Thus, proving a *single* point doubling or point addition involves 161 and 230 arithmetic constraints, respectively. Moreover, when these gadgets are iteratively used to prove just *one* point multiplication with a 128-bit scalar in (4), they dramatically increase the number of arithmetic constraints to 76834.

To avoid the need for creating costly arithmetic constraints for proving modulo n_2 , vPIN employs two correlated curves E_1, E_2 for CP-SNARK and AHE, respectively, by implementing a so-called curve embedding technique [47], [48], [49]. Specifically, we find a custom curve for E_2 such that its base field size equals the order of E_1 , i.e., $n_2 = q_1$. This allows the AHE homomorphic evaluation to be directly captured in the CP-SNARK proving circuits, eliminating the need for creating constraints for proving modulo operations. As a result, the set of arithmetic constraints is reduced, leading to more efficient proving computation, verification, and proof size.

2) *Commitment*: Given a CNN model \mathbf{W} with three sets of parameters (including convolutional filter \mathbf{F} , and weights $\hat{\mathbf{W}}$ and biases $\hat{\mathbf{b}}$ for FC layer), the server commits to \mathbf{W} using the commitment protocol of the back-end CP-SNARK, and publishes the commitment cm to the client (see Figure 6 in Appendix §B).

3) *Encryption*: In vPIN, the client encrypts data sample \mathbf{X}' before sending it to the server for inference. As \mathbf{X}' can be real numbers in practice, vPIN makes use of fixed-point representation to encode \mathbf{X}' as elements in \mathbb{Z}_p for AHE encryption. For each value $\mathbf{X}'[i, j] \in \mathbb{R}$, the client computes its two’s complement fixed-point representation and encrypts it with AHE as $\llbracket C[i, j] \rrbracket_2 \leftarrow \text{AHE.Enc}(\text{pk}, \mathbf{X}[i, j])$, where $\mathbf{X}[i, j] = \mathbf{X}'[i, j] \cdot 2^f$, and f is a system parameter indicating the number of fractional bits (e.g., $f = 16$) in the fixed-point representation (Figure 6). To this end, the client sends the encrypted sample $\llbracket C \rrbracket_2$ to the server for inference evaluation.

4) *Inference*: We present how the server evaluates the CNN inference on the encrypted sample and generates the corresponding proof. Intuitively, vPIN realizes the privacy-preserving CNN inference via additive homomorphic properties of AHE, while the proof is generated by creating arithmetic circuits with EC gadgets introduced in §IV-A. vPIN follows the standard CNN inference computation, which consists of a sequence of operations in the convolutional layer, average pooling, FC layers, and activation layers as follows.

Convolutional Layer. The server first computes $\llbracket \mathbf{A} \rrbracket_2 = \llbracket \mathbf{F} * \mathbf{C} \rrbracket_2$, the convolution between its convolution filter \mathbf{F} of size $k \times k$ and the client sample $\llbracket C \rrbracket_2$ of size $n \times m$ with a stride size \hat{s} by evaluating the homomorphic dot products as

$$\llbracket \mathbf{A}[i, j] \rrbracket_2 = \sum_{i'=0}^{k-1} \sum_{j'=0}^{k-1} \mathbf{F}[i', j'] \cdot \llbracket C[i \cdot \hat{s} + i', j \cdot \hat{s} + j'] \rrbracket_2 \quad (6)$$

for $i \in [0, n']$ and $j \in [0, m']$, where $n' = (((n - k)/\hat{s}) + 1)$ and $m' = (((m - k)/\hat{s}) + 1)$.

Activation Layer. In the standard CNN, after convolution, the next step is to apply an activation function. Since the activation

function is generally non-linear, it cannot be evaluated with AHE. Therefore, in vPIN, we delegate the evaluation of the activation function to the client by having the server transmit the encrypted convolution evaluation. Another important aspect of having such a client-server interaction is to handle the restricted plaintext size of AHE, particularly the exponential ElGamal. Specifically, the convolution output can be up to 35 bits due to dot product operations between the server model and the client sample. Once this output is used for next-layer evaluation, the result can grow up to a size (e.g., >80 bits) that cannot be decrypted by the discrete log algorithm. To handle this issue, in vPIN, after each layer evaluation, the server will send the result to the client so that she can perform a truncation to keep the plaintext size within the decryptable range. In the activation layer, the interaction works as follows.

Let $[[\mathbf{A}]]_2 = [[\mathbf{F} * \mathbf{C}]]_2$ be the encrypted convolution evaluation. In vPIN, for simplicity, we use ReLU as the activation function (i.e., $a' \leftarrow \text{ReLU}(a)$, where $a' = \max(0, a)$ for each $a \in \mathbf{A}$). However, other activation functions such as Sigmoid, Tanh, Swish, and Mish can also be employed effectively. To evaluate ReLU, the server sends $[[\mathbf{A}]]_2$ to the client. For each $[[a]]_2 \in [[\mathbf{A}]]_2$, the client first decrypts it to obtain the value a and then evaluates the ReLU function by sending back to the server either $[[a']]_2 = [[0]]_2$ if $a \leq 0$ or $[[a']]_2 = [[a^*]]_2$ if $a > 0$, where $a^* = a/2^\zeta$ is the f -bit truncated value of a , and ζ is the number of truncated bits. To this end, the server obtains the encrypted ReLU evaluation. We represent our TReLU activation function in Appendix §B, Figure 5.

Pooling Layer. Let $[[\mathbf{A}']]_2$ be the encrypted output of the activation. The next step is to apply a pooling layer on $[[\mathbf{A}']]_2$. Since $[[\mathbf{A}']]_2$ is an AHE cipher, we opt for a linear pooling function (i.e., average pooling) so that it can be evaluated homomorphically by the server. The server computes the average pooling with the $\hat{k} \times \hat{k}$ window as

$$[[\mathbf{B}[i, j]]]_2 = \frac{1}{\hat{k}^2} \sum_{i'=0}^{\hat{k}-1} \sum_{j'=0}^{\hat{k}-1} [[\mathbf{A}'][i \cdot \hat{k} + i', j \cdot \hat{k} + j']]_2 \quad (7)$$

for $i \in [0, n']$ and $j \in [0, m']$.

In each step of the average pooling computation, the server slides a $\hat{k} \times \hat{k}$ window across the input $[[\mathbf{A}']]_2$. At each step, the server computes the homomorphic sum of the window's elements and obtains the average by multiplying it with the fixed-point representation of $1/\hat{k}^2$.

FC Layer. Let $[[\mathbf{d}]]$ be the output of average pooling flattened by $[[\mathbf{d}[i \cdot \hat{n} + j]]]_2 = [[\mathbf{B}[i, j]]]_2$ for $i \in [0, \hat{n}]$ and $j \in [0, \hat{m}]$, where $\hat{n} \times \hat{m}$ denotes $[[\mathbf{B}]]_2$ dimensions. However, since the $\hat{\mathbf{b}}$ values are real numbers, the server first computes the fixed-point representation for each value $\hat{\mathbf{b}}[i]$ and encrypts it with AHE as $[[\mathbf{b}[i]]]_2 \leftarrow \text{AHE.Enc}(\text{pk}, \hat{\mathbf{b}}[i])$ (lines 28-29). Next, the server computes the FC layer with an input size of g and an output size of h . Hence, the server performs homomorphic additive sum on these encrypted bias elements $[[\mathbf{b}]]_2$ along with the result obtained from the point multiplication, resulting in

the inference result $[[\mathbf{t}]]_2$ as

$$[[\mathbf{t}[i]]]_2 = \left(\sum_{j=0}^g \hat{\mathbf{W}}^T[i, j] \cdot [[\mathbf{d}[j]]]_2 \right) + [[\mathbf{b}[i]]]_2 \quad (8)$$

for $i \in [0, h]$.

If there are multiple FC layers, the subsequent step between each FC layer is to compute the TReLU function where the operation is similar to the first activation layer.

Proving Convolutional Layer Computation. As the client sample is encrypted, the convolutional layer comprises two main operations including EC point multiplication and EC point addition. Thus, to prove the convolution layer, we can employ PtAdd and PtMul gadgets to generate the corresponding arithmetic constraints. However, since (6) incurs $O(n^2 \cdot k^2)$ EC point multiplications and $O(n^2 \cdot k^2)$ EC point additions to compute $[[\mathbf{A}]]_2$ (assume $m = n$ and \hat{s} is small constant), simply proving each point operation with an EC gadget will result in a significant cost.

To reduce the overhead, the high-level idea is to flatten components in the convolution layer and then apply the random linear combination technique [50]. Specifically, each convolution iteration by (6) applies a sliding window of size $k \times k$ to $[[\mathbf{C}]]_2$ to extract k^2 elements in $[[\mathbf{C}]]_2$ for dot product computation with the filter \mathbf{F} . First, we flatten each of such windows to a vector of size k^2 , and then form a matrix $[[\hat{\mathbf{C}}]]_2$ that contains all the flattened vectors. Specifically, let $n' = ((n-k)/\hat{s} + 1)$, $m' = ((m-k)/\hat{s} + 1)$ be convolution output size, $[[\hat{\mathbf{C}}]]_2$ is a matrix of size $n' \cdot m' \times k^2$ such that, for each $i \in [0, n']$, $j \in [0, m']$, $i' \in [0, k]$, $j' \in [0, k]$,

$$[[\hat{\mathbf{C}}[i \cdot m' + j, i' \cdot k + j']]_2 = [[\mathbf{C}[i \cdot \hat{s} + i', j \cdot \hat{s} + j']]_2$$

Next, we flatten the convolution filter matrix \mathbf{F} to a vector $\hat{\mathbf{f}}$, where $\hat{\mathbf{f}}[i \cdot k + j] = \mathbf{F}[i, j]$ for $i \in [0, k]$, $j \in [0, k]$. Similarly, we flatten the convolution output as $[[\hat{\mathbf{a}}[i \cdot m' + j]]]_2 = [[\mathbf{A}[i, j]]]_2$ for $i \in [0, n']$, $j \in [0, m']$ and then apply the random linear combination with a random challenge γ (chosen by the verifier) to all the flattened components. Specifically, (5) holds for all $i \in [0, n']$ and $j \in [0, m']$ is equivalent iff the following equation holds

$$\sum_{i'=1}^{n' \cdot m'} \gamma^{i'} \cdot [[\hat{\mathbf{a}}[i']]]_2 = \sum_{j'=1}^{k^2} \left(\sum_{i'=1}^{n' \cdot m'} \gamma^{i'} \cdot [[\hat{\mathbf{C}}[i']]]_2 \right)^T \cdot \hat{\mathbf{f}}[j'] \quad (9)$$

We can see that the number of EC point multiplications and EC point additions in (9) is reduced from $O(n^2 \cdot k^2)$ to $O(k^2)$.

Proving Average Pooling. In vPIN, the average pooling only computes the homomorphic sum of encrypted values followed by multiplying with a public window size parameter (i.e., $\hat{k}^{-2} \in \mathbb{Z}_{q_1}$). Therefore, it suffices to prove this layer by employing PtAdd gadgets for arithmetic constraint representation in (7).

Proving FC Layer. This layer incurs EC point additions and multiplications. Therefore, we can use PtAdd and PtMul gadgets to represent corresponding arithmetic constraints. Nevertheless, simply using EC gadget to prove (8) will be costly since it incurs $O(g \cdot h)$ EC point additions and multiplications to compute $[[\mathbf{t}]]_2$, where g, h indicates the size of the FC layer

input and output, respectively.

To reduce the number of constraints in proving the FC layer, we employ the random linear combination similar to the proof of the convolution layer. However, unlike the convolution layer, we do not need to flatten the weight matrix $\hat{\mathbf{W}}$ in the FC layer before applying the random linear combination. This is because the convolution layer involves multiple matrix multiplications between the filter $\hat{\mathbf{f}}$ and the (small) windowed inputs $\llbracket \mathbf{C} \rrbracket_2$. To perform an efficient random linear combination on the convolution, each window is flattened and formed into a big matrix $\llbracket \hat{\mathbf{C}} \rrbracket_2$, enabling a single matrix multiplication between the filter $\hat{\mathbf{f}}$ and $\llbracket \hat{\mathbf{C}} \rrbracket_2$. Since the FC layer incurs only a single matrix multiplication between the weight $\hat{\mathbf{W}}$ and the output of the average pooling $\llbracket \mathbf{d} \rrbracket_2$, the flattening is not required. Let γ' be a random challenge chosen by the verifier. The FC computation in (8) holds if the following equation holds

$$\sum_{i'=1}^h \gamma'^{i'} \cdot \llbracket \mathbf{t}[i'] \rrbracket_2 = \sum_{j'=1}^g \left(\sum_{i'=1}^h \gamma'^{i'} \cdot \hat{\mathbf{W}}^T[i'] \right) \cdot \llbracket \mathbf{d}[j'] \rrbracket_2 \quad (10)$$

In (10), the number of constraints for EC point multiplications and additions is reduced from $O(g \cdot h)$ to $O(g)$ and $O(g + h)$, respectively. We present the pseudocode of the vPIN inference procedure in Figure 7 in Appendix §B.

Remark. In our vPIN scheme, the server computes the convolutional, average pooling, and FC layers, while the client performs activation. Thus, the server only proves the correctness of the convolutional, average pooling, and FC layers.

5) *Decryption:* In this procedure, the client receives the encrypted inference and the proof of correct homomorphic evaluation of convolution, pooling, and FC layers with respect to the server's committed model. The client verifies the proof, and, if the proof is valid, she decrypts the encrypted inference and obtains the final result (see Figure 8 in Appendix §B).

V. ANALYSIS

Complexity. Let $k \times k$ be the filter dimension in the convolutional layer, $n \times m$ be the dimension of the client data sample (for simplicity, we assume $m = n$), and \hat{s} be the stride size of the convolution window. Let $\hat{k} \times \hat{k}$ be the window dimension in the average pooling layer and g, h be the input and output size of the FC layer. In the convolutional layer, vPIN incurs $k^2 = O(k^2)$ point multiplications and $k^2 - 1 = O(k^2)$ point additions to prove the convolution layer (given \hat{s} as small constant), compared with $O(n^2 \cdot k^2)$ point multiplications and $O(n^2 \cdot k^2)$ point additions in the baseline approach that hardcodes the convolution to the proving circuit. vPIN incurs $(\hat{k}^2 - 1)((n - k)/\hat{s} + 1)^2/\hat{k}^2 = O((n + k)^2)$ point additions to prove pooling layer (with the average pooling). In the FC layer, vPIN requires $g = O(g)$ point multiplications and $(g - 1) + h = O(g + h)$ point additions compared with $O(g \cdot h)$ point multiplications and additions in the baseline. In overall, the complexity of vPIN is $O(k^2 + g)$ point multiplications and $O((n + k)^2 + g + h)$ point additions (Table I).

Security. We state the security of vPIN as follows.

Theorem 1. Assuming AHE is IND-CPA secure by Definition 3 and the back-end CP-SNARK is secure by Definition 1, vPIN is a privacy-preserving and verifiable ML inference by Definition 2.

Proof. See Appendix §C. □

VI. EXPERIMENTAL EVALUATION

A. Implementation

We fully implemented our vPIN scheme in Python and Rust with ≈ 5200 lines of code. We employed the `python-ecdsa` library [51] to generate cryptographic keys based on the EC. We used the standard Python `socket` for client-server communication and employed Python's `hmac` and `hashlib` cryptographic libraries to implement pseudo-random functions (PRFs) for random linear combinations. We implemented the CNN inference phase for several CNN networks, including LeNet [52], from scratch to obtain all witnesses for generating the proofs and committing to auxiliary witnesses. We also implemented the baby-step giant-step algorithm [53] for computing the EC discrete logarithm in our decryption phase.

We used the Rust `libspartan` library [54] to convert our arithmetic constraints into a rank-1 constraint system (RICS) and implement our underlying CP-SNARK scheme involving witnesses commitment, proof generation, and verification. Specifically, we used `SpartanDL` variant, which internally leveraged Hyrax polynomial commitment [55], and `curve25519-dalek` [56] for EC operations. Our implementation is available at <https://github.com/vt-asaplab/vPIN>.

B. Configuration

Hardware. For the client, we used a local Macbook Pro 2021 with a 3.2 GHz M1 Pro CPU and 16 GB RAM. For the server, we used a server machine with a 48-core Intel CPU (Intel(R) Xeon(R) Platinum 8360Y CPU @ 2.40GHz) and 256 GB of RAM. We used thread-level parallelization in `libspartan` to speed up the proving/verification time. Therefore the experimental results reported here are for multi-thread execution, as specified in their respective sections.

System Parameters. For the curve E_1 , we used the standard curve `curve25519-dalek` in `libspartan` with 128-bit security. E_1 used $y^2 = x^3 + 486662x^2 + x$ with based field $2^{255} - 19$ and prime order $2^{252} + 2774231777372353535851937790883648493$. We generate the parameters for the curve E_2 using the ECB toolkit [57] to ensure the base field of E_2 matches the prime order of E_1 . E_2 used $y^2 = x^3 + \alpha_2x + \beta_2^2$ with based field $2^{252} + 2774231777372353535851937790883648493$ and prime order $2^{252} - 124614587218531604318505012771651942947$.

Dataset. We evaluated the performance of our proposed method on the MNIST dataset. We resized the MNIST dataset

²The base-64 encoding of α_2 is B7gQfOmTdkBeTbfbAw9XyzpLLxAP9Z9EjiYqP2UyG50=
The base-64 encoding of β_2 is CAi4LFqrcPqSXatviSmVBGR+j78B7HY4+UDsbkTKU1Y=

TABLE I: Complexity of vPIN (vs. hardcoding baseline).

	vPIN		Baseline	
	# point mult	# point add	# point mult	# point add
Conv.	$O(k^2)$	$O(k^2)$	$O(n^2 \cdot k^2)$	$O(n^2 \cdot k^2)$
Avg Pool	0	$O((n+k)^2)$	0	$O((n+k)^2)$
FC	$O(g)$	$O(g+h)$	$O(g \cdot h)$	$O(g \cdot h)$
Total	$O(k^2 + g)$	$O((n+k)^2 + g + h)$	$O((n^2 \cdot k^2) + (g \cdot h))$	$O((n^2 \cdot k^2) + (n+k)^2 + (g \cdot h))$

images from 28×28 to 32×32 to be suitable to the selected CNN parameter networks.

CNN Network Parameters. We selected different CNNs labeled as networks A, B, C, D, and E (with the increase of model size and number of parameters), each featuring a single convolutional layer, a pooling layer, two FC layers, and two activation layers. All networks use a 3×3 filter size for the convolutional layer. Networks C, D, and E employ a 2×2 window size for the pooling layer, while networks A and B use a 4×4 window size. All networks consist of two FC layers with the number of neural nodes ranging from 10 to 256 per layer. For networks A and B, the first FC layer has 64 nodes, and ends with 16 and 32 nodes in the output, respectively. For networks C, D, and E, the first FC layer starts with 256 nodes and outputs with 16, 32, and 64 nodes, respectively. Within the second FC layer, networks A and B have 16 and 32 nodes, respectively, whereas networks C, D, and E feature 16, 32, and 64 nodes, respectively. All networks have 10 output nodes.

We also assessed the performance of vPIN with the LeNet network [52]. The LeNet model has a total of 61,706 parameters consisting of 3 convolutional layers, 2 average pooling layers, and 2 FC layers. Specifically, there are 6 feature maps in the first convolutional layer and first average pooling, 16 feature maps in the second convolutional layer and second average pooling, and 120 feature maps in the third convolutional layer.

Counterpart Comparison. To our knowledge, we are the first to propose a privacy-preserving and verifiable CNN inference scheme that fully preserves the privacy of the client’s data sample while ensuring inference verifiability. Therefore, we compared our scheme to two different baseline settings. In the first setting, termed Baseline (w/o CE), we directly hardcode the CNN operations that we aim to prove into the arithmetic circuit. For the latter, named Baseline (w/CE), we use the EC Curve Embedding but lack the probabilistic matrix multiplication check. This involves constructing arithmetic constraints for every single computation (including EC point multiplications and EC point additions) in CNN layers. In both settings, we use the same back-end CP-SNARK scheme (i.e., Spartan [14]).

The most closely related works to ours are zkCNN [58] and pvCNN [59]. However, since these schemes offer different functionalities, (e.g., lack of full data privacy) we will only compare our scheme with these works conservatively. We will also discuss the cost of transforming these schemes to achieve full data privacy.

Evaluation Metrics. We benchmark the performance of our scheme and the baseline by measuring their proving time,

verification time, proof size, and inference accuracy.

C. Overall Results

Figure 2 shows the performance of our proposed scheme in proving time, verification time, and proof size compared to the baseline. Our vPIN scheme is 1-6 orders of magnitudes more efficient than the baseline in all metrics. As shown in Figure 2, our proving time ranges from 266 to 1002 sec for all CNN networks 1 to 5, compared to the proving time 27717 to 69756 sec for the Baseline (w/CE), and 612515 to 1545091 sec for the Baseline (w/o CE). Thus, our proving time is 43–104× faster than the Baseline (w/CE) and 951–2304× faster than the Baseline (w/o CE). Our verification time is 15–25× faster than the Baseline (w/CE) and 314–547× faster than the Baseline (w/o CE), taking between 1.7 and 2.8 sec compared to 29 and 70.6 sec and 608 and 1531 sec for the Baseline (w/CE) and Baseline (w/o CE), respectively. In our scheme, the proof size is much smaller than the baseline, ranging from 252 to 367 KB compared to 3133 and 7499 KB for the Baseline (w/CE) and 63950 160797 KB for the Baseline (w/o CE). Thus, the proof size in vPIN is 11–438× times less than the baseline.

Next, we focus on evaluating our proposed scheme on the convolutional layer. This is because optimizing the convolutional layer operations is essential in CNN architecture, as it accounts for the majority of computation operations. Thus, enhancing the efficiency of the convolutional layer operations can significantly improve the overall performance of our CNN.

Convolution. Figure 3 illustrates the comparison between our vPIN scheme and the baseline within the convolutional layer in terms of proving time, verification time, and proof size. We conducted this comparison across various input sizes, ranging from 32×32 to 256×256 , and filter sizes ranging from 3×3 to 7×7 . We set the padding and stride to 1 for the 2D convolutional layer throughout the evaluations. With a 256×256 input and a 3×3 filter, the convolutional proving time in our scheme is 27.78 sec, compared to 1565508 sec in the Baseline (w/CE) and 34715697 sec in the Baseline (w/o CE). Thus, our scheme is 56354–1249665× faster in proving. Furthermore, vPIN achieves a verification time of only 0.64 sec and a proof size of 128 KB, compared with the verification time of 1551 sec and the proof size of 162822 KB in the Baseline (w/CE), and 34354 sec and 3605503 KB in the Baseline (w/o CE). This represents a remarkable improvement of 2423–53678× in verification time and 1273–28188× in proof size.

As depicted in Figure 3, enlarging the input size with the same filter does not increase proving time, verification time,

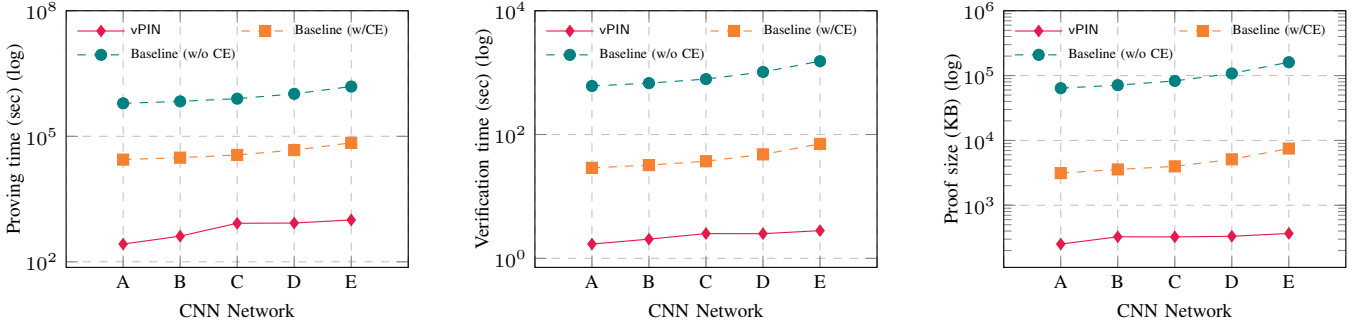


Fig. 2: Performance of vPIN and the baselines on different CNN networks (with increasing # parameters)

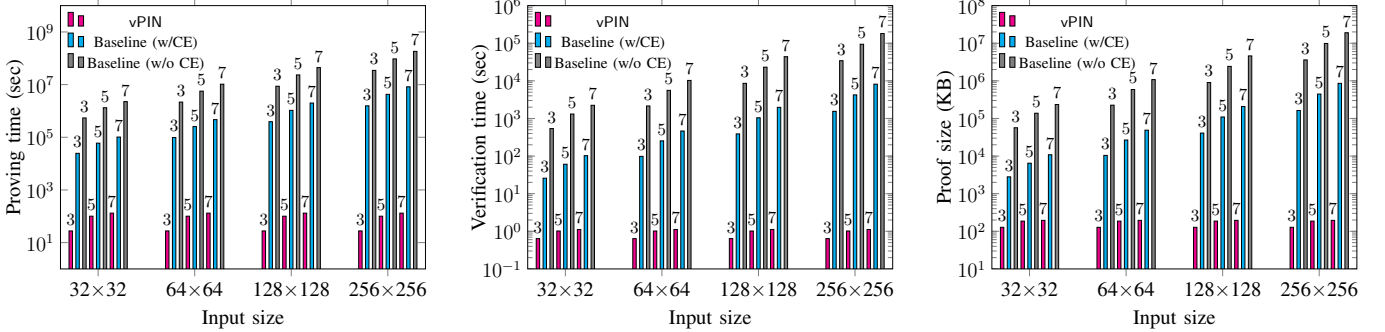


Fig. 3: Performance of vPIN and the baselines for a single convolution

or proof size in our scheme. This is because in vPIN each depends solely on the filter dimension due to random linear combinations. Specifically, for a convolutional layer with a 7×7 filter, our scheme takes 132 sec to prove, 1.12 sec to verify, and produces a proof size of 196 KB across input sizes ranging from 32×32 to 256×256 . In contrast, the baseline takes significantly longer to prove and verify the correctness of larger input sizes as well as the proof size. For instance, Baseline (w/CE) takes 102071 to 8258556 sec, and Baseline (w/o CE) takes 2261884 to 183196050 sec to prove a convolutional layer with a 7×7 filter for input sizes ranging from 32×32 to 256×256 . Similarly, the verification time and proof size range from 103 to 8173 seconds and 10854 to 857850 KB for the Baseline (w/CE), and 2240 to 181280 sec and 235234 to 19024916 KB for the Baseline (w/o CE), respectively.

Within the convolutional layer, the proving and verification times, as well as the proof size in vPIN, increase only slightly with the filter size, for a fixed input size. For example, for a 32×32 input and filter sizes ranging from 3×3 to 7×7 , our scheme takes between 27.8 and 132 sec to generate a proof and between 0.64 and 1.12 sec to verify the proof, with the proof size ranging between 128 and 196 KB. In contrast, the proving and verification times, as well as the proof size in the baseline, increase significantly with the filter size. For a 32×32 input and filter sizes ranging from 3×3 to 7×7 , the Baseline (w/CE) takes between 24574 and 102071 sec to generate a proof, between 25.9 and 103 seconds to verify the proof, and the proof size ranges from 2807 to 10854 KB. Meanwhile, the Baseline (w/o CE) takes 542636 to 2261884 sec and 539

to 2240 sec to generate and verify a proof, with proof sizes ranging from 56693 to 235234 KB. This shows that our scheme is $775\text{--}19519 \times$ faster in proving, $40\text{--}2000 \times$ faster in verifying, and the proof size in our scheme is $22\text{--}1201 \times$ less than that of the baseline when the input size is 32×32 and the filter sizes range from 3×3 to 7×7 .

Experiments with LeNet. We compared the performance of our vPIN scheme against the baselines on LeNet [52] to explore our scheme’s performance within a real network setting. As shown in Table II, our vPIN scheme is faster and more efficient at proving, verifying, and proof size. Specifically, our proving time is 10699 sec for 7508 point multiplications and 16864 point additions, compared to the Baseline (w/CE) and Baseline (w/o CE), which take days (241 to 5254 hours) for 652040 point multiplications and 637248 point additions. This makes our proving time $81\text{--}1768 \times$ faster than the baseline. For verification time, our scheme only takes 15.9 sec, while the Baseline (w/CE) and Baseline (w/o CE) take 866.6 and 17883 sec, respectively. Lastly, our proof size is 2339 KB, smaller than Baseline (w/CE) and Baseline (w/o CE), which are 91510 and 1991995 KB respectively. Thus, it is $39\text{--}852 \times$ smaller than the baseline.

In Table II, the increased overhead in the third convolutional layer of vPIN is mainly due to computing 120 feature maps. This substantially impacts the overall overhead of the scheme.

Proving Circuit Size. To better understand the proving times in Figure 2 and Figure 3, we present in Table III the number of arithmetic constraints required for proving n EC point multiplications and n EC point additions within R1CS in

TABLE II: Performance of our vPIN scheme on LeNet [52]

	vPIN			Baseline (w/CE)			Baseline (w/o CE)		
	\mathcal{P} (s)	\mathcal{V} (s)	III (KB)	\mathcal{P} (s)	\mathcal{V} (s)	III (KB)	\mathcal{P} (s)	\mathcal{V} (s)	III (KB)
1 st Conv.	417	1.8	298	312225	310.5	32677	6828361	6387	696674
1 st Avg Pool	34	0.6	104	34	0.6	104	713.3	12.1	2302
2 nd Conv.	1538	3.2	477	398215	395.5	41607	8617373	8211	916186
2 nd Avg Pool	16	0.4	83	16	0.4	83	327.2	8.7	1714
3 rd Conv.	8043	6.6	856	127507	127.7	13496	2793806	2603	298693
1 st FC	401	1.8	298	26867	28.1	3045	570730	583.3	65563
2 nd FC	250	1.5	223	2344	3.8	498	49299	78.1	10863
Total	10699	15.9	2339	867207	866.6	91510	18914609	17883	1991995

TABLE III: Number of RICS constraints for n EC point multiplications and point additions.

Operations	# Constraints in vPIN / Baseline (w/CE)	# Constraints in Baseline (w/o CE)
EC point mult	$3464 \cdot n$	$76834 \cdot n$
EC point add	$10 \cdot n$	$230 \cdot n$

TABLE IV: Number of RICS constraints in LeNet [52]

Operations	# Constraints in vPIN	# Constraints in Baseline (w/CE)	# Constraints in Baseline (w/o CE)
EC point mult	26,007,712	2,258,666,560	50,098,841,360
EC point add	168,640	6,372,480	146,567,040
Total	26,176,352	2,265,039,040	50,245,408,400

both vPIN and the baseline. In vPIN and Baseline (w/CE), a *single* EC point multiplication and EC point addition requires 3464 and 10 arithmetic constraints, respectively. Meanwhile, Baseline (w/o CE) requires 76834 and 230 constraints to prove the same operations. Since the proving time scales linearly with the number of RICS constraints, performing one EC point multiplication consumes more time compared to one EC point addition. This is because proving a single EC point multiplication with a 128-bit scalar involves iterative calls to PtAdd and PtDbl gadgets. Thus, due to the 128-bit random challenge used in the random linear combination, EC point multiplication is more resource-intensive compared to the highly efficient EC point addition, which only requires 10 constraints in vPIN.

In Table IV, we compare the total number of arithmetic constraints required for proving the LeNet model. Specifically, with vPIN, the total number of arithmetic constraints needed to prove all EC point multiplications and additions for LeNet layers is 26.2 million, compared to 2265 million and 50245 million in Baseline (w/CE) and Baseline (w/o CE), respectively. Thus, vPIN requires 86–1918 \times fewer constraints to prove the LeNet model compared to the baselines.

Accuracy. We assess the impact of fixed-point representation on the inference accuracy of the LeNet model on MNIST, as this is what we used in vPIN. In the original non-secure setting with floating-point data and model parameters, the

LeNet model achieved 97.87% accuracy. When using fixed-point representation and truncation after each layer to keep output within a decryptable range (e.g., ≤ 35 bits) as in vPIN, the accuracy slightly dropped to 97.74%. This decrease (e.g., 0.13%) was expected due to the potential precision loss when converting model parameters and data samples to fixed-point representation and applying truncation.

Experiments with CIFAR-10. We further evaluate the performance of vPIN on the LeNet model using CIFAR-10 as the color image dataset. Unlike MNIST which consists of grayscale images with a single channel, CIFAR-10 images have three channels (e.g., RGB). This requires additional parameters in the first convolutional layer, resulting in an increase in the number of point multiplications and point additions from 7508 to 8108 and from 16864 to 36256, respectively, for the CIFAR-10 dataset compared to MNIST. Consequently, for the CIFAR-10 dataset, vPIN requires 11951 sec for proving time, 18 sec for verification time, and generates a proof size of 2611 KB. In comparison, Baseline (w/CE) requires a proving time of 1778111 sec (resp. 37068924 sec for Baseline (w/o CE)), a verification time of 1768.1 sec (resp. 37314 sec for Baseline (w/o CE)), and produces a proof size of 186194 KB (resp. 3902027 KB for Baseline (w/o CE)). Thus, vPIN is 71–149 \times more efficient than Baseline (w/CE) and 1494–3102 \times more efficient than Baseline (w/o CE).

Discussion. In vPIN, we aim to achieve client data privacy protection using AHE, as well as CNN inference verifiability through CP-SNARK. There are two relevant prior works, zkCNN [58] and pvCNN [59], both focusing on CNN inference verifiability with Commit-and-Prove zero-knowledge SNARK (CP-zkSNARK). However, unlike vPIN, they do not offer full privacy for client data and CNN inference verifiability simultaneously. Specifically, zkCNN [58] is a zero-knowledge CNN scheme that only protects the privacy of the CNN parameters without preserving the privacy of the client’s data. The core technique in zkCNN is the new sumcheck protocol for fast Fourier transform (FFT) and doubly efficient interactive proofs for proving the CNN inference, particularly the convolution and matrix multiplication operations within the FC layers. Although FFT permits fast proving of convolution operations on two plaintext inputs (client sample and server model), it may be challenging to apply FFT to the context

where the client sample is homomorphically encrypted since the HE ciphertexts operate on somewhat unfriendly FFT algebraic group structures [60], [61].

pvCNN [59] is a privacy-preserving CNN inference scheme that offers verifiability and client data privacy. Although pvCNN uses similar building blocks as vPIN including HE (fully vs. partially in vPIN) and (CP-zkSNARK vs. CP-SNARK in vPIN), unlike vPIN, pvCNN only offers partial privacy for the client sample. This is because, in pvCNN, the CNN network is divided into two parts: PriorNet and LaterNet. In PriorNet, the CNN developer (i.e., the server in our case) evaluates a subset of CNN layers on the client ciphertext and generates a zero-knowledge proof for this portion. In LaterNet, the encrypted evaluation of PriorNet is decrypted to a third party to continue the inference computation and zero-knowledge proof on the subsequent CNN layers. As the third party learns the evaluation output of PriorNet, therefore, it can infer client data information. Moreover, as the third party has access to a portion of the CNN model of the server (LaterNet), pvCNN only offers partial privacy to the server model (PriorNet privacy). Meanwhile, in vPIN, the client data (as well as inference output) is kept encrypted all the time throughout the CNN inference evaluation. From the performance perspective, pvCNN relies on Fully Homomorphic Encryption (FHE), which is more costly than AHE. Thus, we expect that to make pvCNN achieve the same level of privacy as vPIN, one has to construct complicated proving circuits for FHE operations and, therefore, its concrete performance will be significantly slower than vPIN.

VII. RELATED WORK

Privacy-Preserving ML. PPML enables the deployment of machine learning models while preserving the privacy of sensitive information in the training/testing data and model parameters. HE [17], MPC [18], and Differential Privacy [62], [63], or Trusted Execution Environment (TEE) such as Intel-SGX [64] are the most commonly used techniques for PPML. PPML research covers both the training and inference phases. A variety of studies focus on PPML in training schemes for machine learning algorithms such as linear regression [26], [24], logistic regression [25], [26], [65], [19], [66], Decision Trees (DT) [67], [68], Support Vector Machines (SVM) [69], Neural Networks (NN) [26], and k-means clustering algorithms [27], [70]. Other research explores PPML techniques for the inference phase (e.g., [25], [22], [23], [71], [20], [72], [21], [73], [74], [75]). Despite significant advancements, a common limitation in existing approaches is the lack of a robust mechanism for guaranteeing computational integrity. This limitation can leave vulnerabilities in the integrity of outcomes, especially when clients rely on privacy-preserving computations without the ability to verify the computation’s correctness. Moreover, while MPC-based schemes offer potential solutions, they may face limitations in adapting to the MLaaS setting due to their reliance distributed computation among two or more entities. SecureDL [76] offers some insights into this challenge with probabilistic verifiability. In SecureDL, a client encrypts her pre-trained model and data samples using Leveled

Homomorphic Encryption and delegates them to a cloud server for inference computation. SecureDL achieves verifiability by enabling the client to use some sensitive-data to check whether the server processes encrypted data with the actual encrypted model. However, this approach does not provide provable verifiability and relies instead on probabilistic methods.

Verifiable ML. Verifiable ML ensures the verifiability of ML algorithm computations by providing provable security. It allows a client to delegate a machine learning task (e.g., training, inference), to a server, and then focus only on verifying the correctness of the training/inference output. Cryptographic proofs, including Verifiable Computation (VC) protocols [8], [9] and zero-knowledge proofs (ZKPs) [10], [11], [12], [13], [14], [15], [16] or TEEs [64], are the core techniques for verifiable ML. Verifiable ML can be categorized into trusted-setup and trustless schemes. Trusted-setup schemes rely on a trusted third party (TTP) to generate a Common Reference String (CRS) such as Gennaro, Gentry, Parno, and Raykova (GGPR) [11], which introduces potential security vulnerabilities and trust assumptions. In contrast, trustless schemes such as Bulletproofs [16] and Spartan [14] eliminate the need for a TTP or CRS, enhancing security and removing trust assumptions. Research in verifiable ML includes various machine learning algorithms like deep neural networks (DNN) inference [6], linear regression [7], [77], NN [7], and DT training [7]. Some verifiable ML research incorporates zero-knowledge property across different machine learning algorithms, including DT [78], SVM [79], [80], and DNN [58], [81], [82], [83], [84]. Despite their benefits, verifiable ML schemes may not fully preserve the privacy of client data samples during inference, potentially revealing private information from client data. A closely related work to vPIN is pvCNN [59], which focuses on privacy preservation within specific CNN layers and ensures inference integrity. However, it lacks full client data privacy, allowing a third party to infer client data. pvCNN employs trusted-setup ZKPs to generate proofs for targeted CNN inference layers using a CRS.

VIII. CONCLUSION AND FUTURE WORK

We presented vPIN, a new privacy-preserving and verifiable CNN scheme allowing clients to securely delegate their CNN inference computations on encrypted data to an MLaaS. The server processes the CNN inference for the client’s encrypted data sample while providing proof of correct inference computations. vPIN seamlessly integrates HE and VC protocols, ensuring full privacy for client data and computation integrity. vPIN makes use of several optimization techniques including curve embedding and probabilistic matrix multiplication to reduce the proving circuit size by a few orders of magnitude.

While vPIN offers inference verifiability and client privacy, there are still significant performance challenges to be addressed to make it more practical. Specifically, vPIN requires client-server interaction to handle non-linear functions. Furthermore, the proving and verification time in vPIN is still high, especially when applied to complicated models with millions of model

parameters. Finally, an effective CNN inference pipeline generally consists of multiple processing stages (e.g., convolution, activation, pooling, and FC), which may require the server to re-prove the entire inference pipeline in case of system failures during inference. Therefore, our future work will seek effective strategies to address the aforementioned challenges. We will explore techniques that allow the evaluation of non-linear operations directly on the server thereby, mitigating client-server interaction. To improve the processing delay, we will seek hardware acceleration techniques (e.g., GPU). Finally, emerging cryptographic techniques such as Incrementally Verifiable Computation [85] may be useful for the server to resume proving continuing phases in the inference pipeline in case of system failures. We leave the exploration of these techniques in our future work.

ACKNOWLEDGMENT

The authors thank the anonymous reviewers for their insightful comments and constructive feedback to improve the quality of this work. This work was supported in part by an unrestricted gift from Robert Bosch, 4-VA, and the Commonwealth Cyber Initiative (CCI), an investment in the advancement of cyber R&D, innovation, and workforce development. For more information about CCI, visit www.cyberinitiative.org

REFERENCES

- [1] Microsoft, "Azure ai services," <https://azure.microsoft.com/en-us/products/ai-services>, [n.d.].
- [2] Google, "Google cloud ai platform," <https://cloud.google.com/products/ai>, [n.d.].
- [3] Amazon, "Amazon web services," <https://aws.amazon.com/>, [n.d.].
- [4] FacePlusPlus, "Faceplusplus body detection," <https://www.faceplusplus.com/body-detection/>, [n.d.].
- [5] Clarifai, "Clarifai computer vision services," <https://www.clarifai.com/models/celebrity-face-recognition>, [n.d.].
- [6] Z. Ghodsi, T. Gu, and S. Garg, "Safetynets: Verifiable execution of deep neural networks on an untrusted cloud," *Advances in Neural Information Processing Systems*, vol. 30, 2017.
- [7] L. Zhao, Q. Wang, C. Wang, Q. Li, C. Shen, and B. Feng, "Veriml: Enabling integrity assurances and fair payments for machine learning as a service," *IEEE Transactions on Parallel and Distributed Systems*, vol. 32, no. 10, pp. 2524–2540, 2021.
- [8] V. Vu, S. Setty, A. J. Blumberg, and M. Walfish, "A hybrid architecture for interactive verifiable computation," in *2013 IEEE Symposium on Security and Privacy*. IEEE, 2013, pp. 223–237.
- [9] G. Cormode, J. Thaler, and K. Yi, "Verifying computations with streaming interactive proofs," *arXiv preprint arXiv:1109.6882*, 2011.
- [10] M. Campanelli, D. Fiore, and A. Querol, "Legosnark: Modular design and composition of succinct zero-knowledge proofs," in *Proceedings of the 2019 ACM SIGSAC Conference on Computer and Communications Security*, 2019, pp. 2075–2092.
- [11] R. Gennaro, C. Gentry, B. Parno, and M. Raykova, "Quadratic span programs and succinct nizks without peps," in *Advances in Cryptology—EUROCRYPT 2013: 32nd Annual International Conference on the Theory and Applications of Cryptographic Techniques, Athens, Greece, May 26-30, 2013. Proceedings 32*. Springer, 2013, pp. 626–645.
- [12] S. Goldwasser, Y. T. Kalai, and G. N. Rothblum, "Delegating computation: interactive proofs for muggles," *Journal of the ACM (JACM)*, vol. 62, no. 4, pp. 1–64, 2015.
- [13] B. Parno, J. Howell, C. Gentry, and M. Raykova, "Pinocchio: Nearly practical verifiable computation," *Communications of the ACM*, vol. 59, no. 2, pp. 103–112, 2016.
- [14] S. Setty, "Spartan: Efficient and general-purpose zkSNARKs without trusted setup," in *Annual International Cryptology Conference*. Springer, 2020, pp. 704–737.
- [15] J. Groth, "Short pairing-based non-interactive zero-knowledge arguments," in *Advances in Cryptology-ASIACRYPT 2010: 16th International Conference on the Theory and Application of Cryptology and Information Security, Singapore, December 5-9, 2010. Proceedings 16*. Springer, 2010, pp. 321–340.
- [16] B. Bünz, J. Bootle, D. Boneh, A. Poelstra, P. Wuille, and G. Maxwell, "Bulletproofs: Short proofs for confidential transactions and more," in *2018 IEEE symposium on security and privacy (SP)*. IEEE, 2018, pp. 315–334.
- [17] C. Gentry, *A fully homomorphic encryption scheme*. Stanford university, 2009.
- [18] R. Cramer, I. B. Damgård *et al.*, *Secure multiparty computation*. Cambridge University Press, 2015.
- [19] C. Bonte and F. Vercauteren, "Privacy-preserving logistic regression training," *BMC medical genomics*, vol. 11, pp. 13–21, 2018.
- [20] R. Dathathri, O. Saarikivi, H. Chen, K. Laine, K. Lauter, S. Maleki, M. Musuvathi, and T. Mytkowicz, "Chet: an optimizing compiler for fully-homomorphic neural-network inferencing," in *Proceedings of the 40th ACM SIGPLAN conference on programming language design and implementation*, 2019, pp. 142–156.
- [21] R. Gilad-Bachrach, N. Dowlin, K. Laine, K. Lauter, M. Naehrig, and J. Wernsing, "Cryptonets: Applying neural networks to encrypted data with high throughput and accuracy," in *International conference on machine learning*. PMLR, 2016, pp. 201–210.
- [22] C. Juvekar, V. Vaikuntanathan, and A. Chandrakasan, "{GAZELLE}: A low latency framework for secure neural network inference," in *27th USENIX Security Symposium (USENIX Security 18)*, 2018, pp. 1651–1669.
- [23] J. Liu, M. Juuti, Y. Lu, and N. Asokan, "Oblivious neural network predictions via miniomn transformations," in *Proceedings of the 2017 ACM SIGSAC conference on computer and communications security*, 2017, pp. 619–631.
- [24] P. Mohassel and Y. Zhang, "Secureml: A system for scalable privacy-preserving machine learning," in *2017 IEEE symposium on security and privacy (SP)*. IEEE, 2017, pp. 19–38.
- [25] N. Koti, M. Pancholi, A. Patra, and A. Suresh, "{SWIFT}: Super-fast and robust {Privacy-Preserving} machine learning," in *30th USENIX Security Symposium (USENIX Security 21)*, 2021, pp. 2651–2668.
- [26] P. Mohassel and P. Rindal, "Aby3: A mixed protocol framework for machine learning," in *Proceedings of the 2018 ACM SIGSAC conference on computer and communications security*, 2018, pp. 35–52.
- [27] P. Bunn and R. Ostrovsky, "Secure two-party k-means clustering," in *Proceedings of the 14th ACM conference on Computer and communications security*, 2007, pp. 486–497.
- [28] V. Chandrasekaran, K. Chaudhuri, I. Giacomelli, S. Jha, and S. Yan, "Exploring connections between active learning and model extraction," in *29th USENIX Security Symposium (USENIX Security 20)*, 2020, pp. 1309–1326.
- [29] F. Tramèr, F. Zhang, A. Juels, M. K. Reiter, and T. Ristenpart, "Stealing machine learning models via prediction {APIs}," in *25th USENIX security symposium (USENIX Security 16)*, 2016, pp. 601–618.
- [30] R. N. Reith, T. Schneider, and O. Tkachenko, "Efficiently stealing your machine learning models," in *Proceedings of the 18th ACM Workshop on Privacy in the Electronic Society*, 2019, pp. 198–210.
- [31] M. Juuti, S. Szyller, S. Marchal, and N. Asokan, "Prada: protecting against dnn model stealing attacks," in *2019 IEEE European Symposium on Security and Privacy (EuroS&P)*. IEEE, 2019, pp. 512–527.
- [32] B. Wang and N. Z. Gong, "Stealing hyperparameters in machine learning," in *2018 IEEE symposium on security and privacy (SP)*. IEEE, 2018, pp. 36–52.
- [33] S. Mariani, F. Zambonelli, A. Tenyi, I. Cano, and J. Roca, "Risk prediction as a service: a dss architecture promoting interoperability and collaboration," in *2019 IEEE 32nd International Symposium on Computer-Based Medical Systems (CBMS)*. IEEE, 2019, pp. 300–305.
- [34] A. Michalas, N. Paladi, and C. Gehrman, "Security aspects of e-health systems migration to the cloud," in *2014 IEEE 16th International Conference on e-Health Networking, Applications and Services (Healthcom)*. IEEE, 2014, pp. 212–218.
- [35] J. Cabrero-Holgueras and S. Pastrana, "Towards realistic privacy-preserving deep learning over encrypted medical data," *Frontiers in Cardiovascular Medicine*, vol. 10, p. 1117360, 2023.
- [36] I. Pereira, A. Madureira, N. Bettencourt, D. Coelho, M. Â. Rebelo, C. Araújo, and D. A. de Oliveira, "A machine learning as a service

- (mlaas) approach to improve marketing success,” in *Informatics*, vol. 11, no. 2. MDPI, 2024, p. 19.
- [37] R. Cramer, R. Gennaro, and B. Schoenmakers, “A secure and optimally efficient multi-authority election scheme,” *European transactions on Telecommunications*, vol. 8, no. 5, pp. 481–490, 1997.
- [38] Y. LeCun, B. Boser, J. S. Denker, D. Henderson, R. E. Howard, W. Hubbard, and L. D. Jackel, “Backpropagation applied to handwritten zip code recognition,” *Neural computation*, vol. 1, no. 4, pp. 541–551, 1989.
- [39] Y. LeCun, L. Bottou, Y. Bengio, and P. Haffner, “Gradient-based learning applied to document recognition,” *Proceedings of the IEEE*, vol. 86, no. 11, pp. 2278–2324, 1998.
- [40] H. Jia, C. A. Choquette-Choo, V. Chandrasekaran, and N. Papernot, “Entangled watermarks as a defense against model extraction,” in *30th USENIX Security Symposium (USENIX Security 21)*, 2021, pp. 1937–1954.
- [41] H. Yu, K. Yang, T. Zhang, Y.-Y. Tsai, T.-Y. Ho, and Y. Jin, “Cloudleak: Large-scale deep learning models stealing through adversarial examples,” in *NDSS*, 2020.
- [42] H. Hu and J. Pang, “Stealing machine learning models: Attacks and countermeasures for generative adversarial networks,” in *Annual Computer Security Applications Conference*, 2021, pp. 1–16.
- [43] M. Mazeika, B. Li, and D. Forsyth, “How to steer your adversary: Targeted and efficient model stealing defenses with gradient redirection,” in *International Conference on Machine Learning*. PMLR, 2022, pp. 15 241–15 254.
- [44] H. Zheng, Q. Ye, H. Hu, C. Fang, and J. Shi, “Bdpl: A boundary differentially private layer against machine learning model extraction attacks,” in *Computer Security–ESORICS 2019: 24th European Symposium on Research in Computer Security, Luxembourg, September 23–27, 2019, Proceedings, Part I 24*. Springer, 2019, pp. 66–83.
- [45] T. Orekondy, B. Schiele, and M. Fritz, “Prediction poisoning: Utility-constrained defenses against model stealing attacks,” in *International Conference on Representation Learning (ICLR) 2020*, 2020.
- [46] A. L. Xiong, B. Chen, Z. Zhang, B. Bünz, B. Fisch, F. Krell, and P. Camacho, “{VeriZexe}: Decentralized private computation with universal setup,” in *32nd USENIX Security Symposium (USENIX Security 23)*, 2023, pp. 4445–4462.
- [47] S. Bowe, A. Chiesa, M. Green, I. Miers, P. Mishra, and H. Wu, “Zexe: Enabling decentralized private computation,” in *2020 IEEE Symposium on Security and Privacy (SP)*. IEEE, 2020, pp. 947–964.
- [48] D. Hopwood, S. Bowe, T. Hornby, N. Wilcox *et al.*, “Zcash protocol specification,” *GitHub: San Francisco, CA, USA*, vol. 4, no. 220, p. 32, 2016.
- [49] S. Steffen, B. Bichsel, R. Baumgartner, and M. Vechev, “Zeestar: Private smart contracts by homomorphic encryption and zero-knowledge proofs,” in *2022 IEEE Symposium on Security and Privacy (SP)*, 2022, pp. 179–197.
- [50] R. Freivalds, “Probabilistic machines can use less running time,” in *IFIP Congress*, 1977, p. 839–842.
- [51] H. Kario and B. Warner, “pure-python ecdsa signature/verification and ecdh key agreement,” <https://github.com/tlsfuzzer/python-ecdsa>, 2021.
- [52] Y. Lecun, L. Bottou, Y. Bengio, and P. Haffner, “Gradient-based learning applied to document recognition,” *Proceedings of the IEEE*, vol. 86, no. 11, pp. 2278–2324, 1998.
- [53] D. Shanks, “Class number, a theory of factorization, and genera,” in *Proc. Symp. Math. Soc.*, 1971, vol. 20, 1971, pp. 415–440.
- [54] S. Setty, “Spartan: High-speed zkSNARKs without trusted setup,” <https://github.com/microsoft/Spartan>, 2020.
- [55] R. S. Wahby, I. Tzialla, A. Shelat, J. Thaler, and M. Walfish, “Doubly-efficient zkSNARKs without trusted setup,” in *2018 IEEE Symposium on Security and Privacy (SP)*. IEEE, 2018, pp. 926–943.
- [56] I. A. Lovecruft and H. d. Valence, “A pure-rust implementation of group operations on ristretto and curve25519,” <https://github.com/dalek-cryptography/curve25519-dalek>, 2020.
- [57] M. Martin, “Elliptic curve builder,” <http://www.ellipsa.eu/public/ecb/ecb.html>, 2015.
- [58] T. Liu, X. Xie, and Y. Zhang, “ZkCNN: Zero knowledge proofs for convolutional neural network predictions and accuracy,” in *Proceedings of the 2021 ACM SIGSAC Conference on Computer and Communications Security*, 2021, pp. 2968–2985.
- [59] J. Weng, J. Weng, G. Tang, A. Yang, M. Li, and J.-N. Liu, “pvcnn: Privacy-preserving and verifiable convolutional neural network testing,” *IEEE Transactions on Information Forensics and Security*, vol. 18, pp. 2218–2233, 2023.
- [60] E. Ben-Sasson, D. Carmon, S. Kopparty, and D. Levit, “Elliptic curve fast fourier transform (ecfft) part i: fast polynomial algorithms over all finite fields,” *arXiv preprint arXiv:2107.08473*, 2021.
- [61] ———, “Scalable and transparent proofs over all large fields, via elliptic curves: (ecfft part ii),” in *Theory of Cryptography Conference*. Springer, 2022, pp. 467–496.
- [62] C. Dwork, “Differential privacy,” in *International colloquium on automata, languages, and programming*. Springer, 2006, pp. 1–12.
- [63] C. Dwork, F. McSherry, K. Nissim, and A. Smith, “Calibrating noise to sensitivity in private data analysis,” in *Theory of Cryptography: Third Theory of Cryptography Conference, TCC 2006, New York, NY, USA, March 4-7, 2006. Proceedings 3*. Springer, 2006, pp. 265–284.
- [64] V. Costan and S. Devadas, “Intel sgx explained,” *Cryptology ePrint Archive*, 2016.
- [65] A. B. Slavkovic, Y. Nardi, and M. M. Tibbits, ““ secure” logistic regression of horizontally and vertically partitioned distributed databases,” in *Seventh IEEE International Conference on Data Mining Workshops (ICDMW 2007)*. IEEE, 2007, pp. 723–728.
- [66] K. Chaudhuri and C. Monteleoni, “Privacy-preserving logistic regression,” *Advances in neural information processing systems*, vol. 21, 2008.
- [67] R. Agrawal and R. Srikant, “Privacy-preserving data mining,” in *Proceedings of the 2000 ACM SIGMOD international conference on Management of data*, 2000, pp. 439–450.
- [68] L. Liu, R. Chen, X. Liu, J. Su, and L. Qiao, “Towards practical privacy-preserving decision tree training and evaluation in the cloud,” *IEEE Transactions on Information Forensics and Security*, vol. 15, pp. 2914–2929, 2020.
- [69] J. Vaidya, H. Yu, and X. Jiang, “Privacy-preserving svm classification,” *Knowledge and Information Systems*, vol. 14, pp. 161–178, 2008.
- [70] G. Jagannathan and R. N. Wright, “Privacy-preserving distributed k-means clustering over arbitrarily partitioned data,” in *Proceedings of the eleventh ACM SIGKDD international conference on Knowledge discovery in data mining*, 2005, pp. 593–599.
- [71] M. S. Riazi, M. Samragh, H. Chen, K. Laine, K. Lauter, and F. Koushanfar, “{XONN}: {XNOR-based} oblivious deep neural network inference,” in *28th USENIX Security Symposium (USENIX Security 19)*, 2019, pp. 1501–1518.
- [72] P. Mishra, R. Lehmkuhl, A. Srinivasan, W. Zheng, and R. A. Popa, “Delphi: A cryptographic inference system for neural networks,” in *Proceedings of the 2020 Workshop on Privacy-Preserving Machine Learning in Practice*, 2020, pp. 27–30.
- [73] E. Hesamifard, H. Takabi, and M. Ghasemi, “Cryptodl: Deep neural networks over encrypted data,” *arXiv preprint arXiv:1711.05189*, 2017.
- [74] A. Brutzkus, R. Gilad-Bachrach, and O. Elisha, “Low latency privacy preserving inference,” in *International Conference on Machine Learning*. PMLR, 2019, pp. 812–821.
- [75] D. Natarajan, A. Loveless, W. Dai, and R. Dreslinski, “Chex-mix: Combining homomorphic encryption with trusted execution environments for two-party oblivious inference in the cloud,” *Cryptology ePrint Archive*, 2021.
- [76] G. Xu, H. Li, H. Ren, J. Sun, S. Xu, J. Ning, H. Yang, K. Yang, and R. H. Deng, “Secure and verifiable inference in deep neural networks,” in *Proceedings of the 36th Annual Computer Security Applications Conference*, 2020, pp. 784–797.
- [77] H. Zhang, P. Gao, J. Yu, J. Lin, and N. N. Xiong, “Machine learning on cloud with blockchain: a secure, verifiable and fair approach to outsource the linear regression,” *IEEE Transactions on Network Science and Engineering*, vol. 9, no. 6, pp. 3956–3967, 2021.
- [78] J. Zhang, Z. Fang, Y. Zhang, and D. Song, “Zero knowledge proofs for decision tree predictions and accuracy,” in *Proceedings of the 2020 ACM SIGSAC Conference on Computer and Communications Security*, 2020, pp. 2039–2053.
- [79] W. Haodi and T. Hoang, “ezdps: An efficient and zero-knowledge machine learning inference pipeline,” in *Proceedings on Privacy Enhancing Technologies*, 2023, pp. 430–448.
- [80] H. Wang, R. Bie, and T. Hoang, “An efficient and zero-knowledge classical machine learning inference pipeline,” *IEEE Transactions on Dependable and Secure Computing*, pp. 1–18, 2024.
- [81] B. Feng, L. Qin, Z. Zhang, Y. Ding, and S. Chu, “Zen: An optimizing compiler for verifiable, zero-knowledge neural network inferences,” *Cryptology ePrint Archive*, 2021.

- [82] S. Lee, H. Ko, J. Kim, and H. Oh, “vcnn: Verifiable convolutional neural network based on zk-snarks,” *Cryptology ePrint Archive*, 2020.
- [83] Y. Fan, B. Xu, L. Zhang, J. Song, A. Zomaya, and K.-C. Li, “Validating the integrity of convolutional neural network predictions based on zero-knowledge proof,” *Information Sciences*, vol. 625, pp. 125–140, 2023.
- [84] C. Weng, K. Yang, X. Xie, J. Katz, and X. Wang, “Mystique: Efficient conversions for {Zero-Knowledge} proofs with applications to machine learning,” in *30th USENIX Security Symposium (USENIX Security 21)*, 2021, pp. 501–518.
- [85] P. Valiant, “Incrementally verifiable computation or proofs of knowledge imply time/space efficiency,” in *Theory of Cryptography: Fifth Theory of Cryptography Conference, TCC 2008, New York, USA, March 19-21, 2008. Proceedings 5*. Springer, 2008, pp. 1–18.

APPENDIX A ADDITIONAL AHE BACKGROUND

We present the correctness and IND-CPA security of AHE as follows.

Correctness. An AHE scheme is correct if for any $\lambda, m_1, m_2 \in \mathbb{Z}_n$ s.t. $(pk, sk) \leftarrow \text{AHE.KeyGen}(1^\lambda)$, it holds that $\Pr[\text{AHE.Dec}(sk, \text{AHE.Enc}(pk, m_1) \boxplus \text{AHE.Enc}(pk, m_2)) = (m_1 + m_2)] = 1$ and $\Pr[\text{AHE.Dec}(sk, m_2 \boxtimes (\text{AHE.Enc}(pk, m_1))) = m_1 \cdot m_2] = 1$.

Definition 3 (IND-CPA Security). Let \mathcal{A} be a PPT adversary and λ be the security parameter. A CPA indistinguishability experiment $\text{Adv}_{\mathcal{A}}^{\text{cpa}}(\lambda)$ between the challenger \mathcal{Q} and \mathcal{A} is as follows

1. \mathcal{Q} executes $(pk, sk) \leftarrow \text{AHE.KeyGen}(1^\lambda)$ and randomly selects a bit $b \xleftarrow{\$} \{0, 1\}$. Then, \mathcal{Q} transmits pk to \mathcal{A} .
2. Repeat the following until the adversary decides to stop:
 - a) $\mathcal{A} \rightarrow \mathcal{Q}$: \mathcal{A} outputs m_0 and m_1 of equal length.
 - b) $\mathcal{Q} \rightarrow \mathcal{A}$: \mathcal{Q} executes $\llbracket C \rrbracket \leftarrow \text{AHE.Enc}(pk, m_b)$.
3. $\mathcal{A} \rightarrow \mathcal{Q}$: \mathcal{A} outputs a bit b' .

If $b' = b$, $\text{Adv}_{\mathcal{A}}^{\text{cpa}}(\lambda) = 1$ (\mathcal{A} succeeds); otherwise $\text{Adv}_{\mathcal{A}}^{\text{cpa}}(\lambda) = 0$. We say AHE is *IND-CPA-secure* if $\Pr[\text{Adv}_{\mathcal{A}}^{\text{cpa}}(\lambda) = 1] \leq 1/2 + \text{negl}(\lambda)$

In Figure 4, we present exponential ElGamal [37] encryption scheme on cyclic group \mathbb{G} . The decryption in exponential ElGamal makes use of a discrete log solver function (discretelog), which takes $\llbracket m \rrbracket \in \mathbb{G}$ as input, and returns m .

```

(pk, sk) ← AHE.KeyGen(1λ):
1: x ←$ ℤq* where q is the prime order of ℚ
2: sk := x
3: pk := ⌊x⌋
4: return (pk, sk)
⌊c⌋ ← AHE.Enc(pk, m):
5: r ←$ ℤq*
6: ⌊c1⌋ = ⌊r⌋
7: ⌊c2⌋ = ⌊m⌋ + r⌊x⌋
8: return ⌊c⌋ := (⌊c1⌋, ⌊c2⌋)
m ← AHE.Dec(sk, ⌊c⌋):
9: parse ⌊c⌋ := (⌊c1⌋, ⌊c2⌋)
10: ⌊s⌋ = x · ⌊c1⌋
11: ⌊m̂⌋ = ⌊c2⌋ + (-1) · ⌊s⌋
12: m ← discretelog(⌊m̂⌋)           ▷ brute-force to find m
13: return m

```

Fig. 4: Exponential ElGamal Encryption

APPENDIX B DETAILED vPIN PROTOCOL

We present the TReLU function in Figure 5, and our detailed scheme protocol in Figure 6, Figure 7, and Figure 8.

```

⌊a'⌋2 ← TReLU(sk, pk, ⌊a⌋2, pp):
1: a ← AHE.Dec(sk, ⌊a⌋2)
2: if a ≤ 0 then
3:   ⌊a'⌋2 := ⌊0⌋2
4: else if a > 0 then
5:   a* := a/2ϕ
6:   ⌊a*⌋2 ← AHE.Enc(pk, a*)
7:   ⌊a'⌋2 := ⌊a*⌋2
8: return ⌊a'⌋2

```

Fig. 5: TReLU function

```

(sk, pk, pp) ← vPIN.Setup(1λ, l):
1: Find E1 be an EC of a base field n1 and a prime order q1
2: Find E2 be an EC of a base field q1 and a prime order q2
3: pp' ← CPS.Setup(1λ)
4: (pk, sk) ← AHE.KeyGen(1λ)
5: pp ← (pp', E1, E2, n1, q1, q2)
6: return (sk, pk, pp)
cm̂ ← vPIN.Comm(W, r, pp):
7: cm̂ ← CPS.Comm(W, r, pp)
8: return cm̂
⌊C⌋2 ← vPIN.Enc(pk, X, pp):
9: for i = 1 to n do ▷ n × m: encrypted data sample dimensions
10:   for j = 1 to m do
11:     ⌊C[i, j]⌋2 ← AHE.Enc(pk, X[i, j])
12: return ⌊C⌋2

```

Fig. 6: Our proposed vPIN (part 1)

APPENDIX C PROOF OF THEOREM 1

We prove the completeness, soundness, and sample and inference privacy of vPIN as follows.

Completeness. In our vPIN scheme (Figure 6, Figure 7, and Figure 8), if the inference result \mathbf{t} and its decryption \mathbf{y} are correct, then vPIN.Dec will not output \perp . The correctness of \mathbf{t} within our vPIN scheme holds due to the completeness property of the back-end CP-SNARK scheme, and the correctness of \mathbf{y} holds due to the correctness and homomorphic properties of the back-end AHE scheme.

Soundness. Let \mathbf{W} be the model parameters, r be the randomness, \mathbf{X} be the client data sample such that $\mathbf{C} \leftarrow \text{vPIN.Enc}(pk, \mathbf{X}, pp)$, $(\pi, \mathbf{t}) \leftarrow \text{vPIN.Infer}(\mathbf{W}, \mathbf{C}, pp)$, and $cm = \text{vPIN.Comm}(\mathbf{W}, r, pp)$. Let $\hat{\mathbf{W}} \neq \mathbf{W}$ be an arbitrary model and $\hat{\mathbf{C}} \neq \mathbf{C}$ be an arbitrary encrypted sample. Let $cm^* \leftarrow \text{vPIN.Comm}(\hat{\mathbf{W}}, r, pp)$ and $(\pi^*, \mathbf{t}^*) \leftarrow \text{vPIN.Infer}(\hat{\mathbf{W}}, \hat{\mathbf{C}}, pp)$. Let \mathcal{F}' be the ideal inference functionality that returns the correct inference result on the input \mathbf{W} and \mathbf{X} . If $\text{vPIN.Dec}(sk, \mathbf{t}^*, cm, \pi^*, pp) \neq \perp$ however

```

 $(\pi, \mathbf{t}) \leftarrow \text{vPIN.Infer}(\mathbf{W}, \llbracket \mathbf{C} \rrbracket_2, \text{pp}):$ 
13: parse  $\mathbf{W} := (\mathbf{F}, \hat{\mathbf{W}}, \hat{\mathbf{b}})$   $\triangleright \mathbf{F}$  : conv. filter,  $\hat{\mathbf{W}}, \hat{\mathbf{b}}$ : FC layer parameters
14:  $n' = ((n - k)/\hat{s}) + 1$   $\triangleright k$  : conv. filter size  $\hat{s}$  : stride size
15:  $m' = ((m - k)/\hat{s}) + 1$ 
16: for  $i = 0$  to  $n'$  do
17:   for  $j = 0$  to  $m'$  do
18:      $\llbracket \mathbf{A}[i, j] \rrbracket_2 = \sum_{i'=0}^{k-1} \sum_{j'=0}^{k-1} \mathbf{F}[i', j'] \cdot \llbracket \mathbf{C}[i \cdot \hat{s} + i', j \cdot \hat{s} + j'] \rrbracket_2$ 
19: Server interacts with the client to compute  $\llbracket \mathbf{A}'[i, j] \rrbracket_2 \leftarrow \text{TReLU}(\text{sk}, \text{pk}, \llbracket \mathbf{A}[i, j] \rrbracket_2, \text{pp})$  for each  $i \in [0, n']$  and  $j \in [0, m']$ .
20: for  $i = 0$  to  $n'$  do
21:   for  $j = 0$  to  $m'$  do
22:      $\llbracket \mathbf{B}[i, j] \rrbracket_2 = \frac{1}{\hat{k}^2} \sum_{i'=0}^{\hat{k}-1} \sum_{j'=0}^{\hat{k}-1} \llbracket \mathbf{A}'[i \cdot \hat{k} + i', j \cdot \hat{k} + j'] \rrbracket_2$   $\triangleright \hat{k}$  : pooling window size
23:  $\hat{n} = n' / \hat{k}$ 
24:  $\hat{m} = m' / \hat{k}$ 
25: for  $i = 0$  to  $\hat{n}$  do
26:   for  $j = 0$  to  $\hat{m}$  do
27:      $\llbracket \mathbf{d}[i \cdot \hat{m} + j] \rrbracket_2 = \llbracket \mathbf{B}[i, j] \rrbracket_2$ 
28: for  $i = 1$  to  $h$  do  $\triangleright h$  : FC layer output size
29:    $\llbracket \mathbf{b}[i] \rrbracket_2 \leftarrow \text{AHE.Enc}(\text{pk}, \hat{\mathbf{b}}[i])$ 
30: for  $i = 1$  to  $h$  do
31:    $\llbracket \mathbf{t}[i] \rrbracket_2 = (\sum_{j=0}^g \hat{\mathbf{W}}^T[i, j] \cdot \llbracket \mathbf{d}[j] \rrbracket_2) + \llbracket \mathbf{b}[i] \rrbracket_2$   $\triangleright g$  : FC layer input size
32: To compute the next FC layers, the server interacts with the client to compute  $\llbracket \mathbf{t}'[i] \rrbracket_2 \leftarrow \text{TReLU}(\text{sk}, \text{pk}, \llbracket \mathbf{t}[i] \rrbracket_2, \text{pp})$  for each  $i \in [0, h]$ .
    The server repeats the process in lines 29 to 32 with the new weight  $\hat{\mathbf{W}}_1$  and bias  $\hat{\mathbf{b}}_1$  parameters.
33: Let  $\phi_{\text{cnn}}, \phi_{\text{pl}}, \phi_{\text{fc}}$  be arithmetic circuits for convolution, pooling, and FC layer, respectively. The server uses PtMul and PtAdd gadgets to
    generate constraints for  $\phi_{\text{cnn}}, \phi_{\text{fc}}$ , and PtAdd to generate constraints for  $\phi_{\text{pl}}$ . Let  $\text{aux}_{\text{cnn}}, \text{aux}_{\text{pl}}, \text{aux}_{\text{fc}}$  be auxiliary witnesses when creating
    arithmetic constraints for  $\phi_{\text{cnn}}, \phi_{\text{pl}}, \phi_{\text{fc}}$ , respectively. The server commits to all auxiliary witnesses as  $\text{cm}' \leftarrow \text{CPS.Comm}(\text{aux}, r_2, \text{pp})$ ,
    where  $\text{aux} = (\text{aux}_{\text{cnn}}, \text{aux}_{\text{pl}}, \text{aux}_{\text{fc}})$  and  $r_2 \xleftarrow{\$} \mathbb{Z}_q^*$ , and creates a proof  $\pi \leftarrow \text{CPS.Prov}(\phi, (\mathbf{F}, \hat{\mathbf{W}}, \hat{\mathbf{b}}, \text{aux}), \text{pp})$ , where  $\phi$  is the merge
    arithmetic circuit consisting of  $\phi_{\text{cnn}}, \phi_{\text{pl}}$ , and  $\phi_{\text{fc}}$ .
34: return  $(\hat{\pi}, \llbracket \mathbf{t} \rrbracket_2)$  where  $\hat{\pi} := (\pi, \text{cm}')$ 

```

Fig. 7: Our proposed vPIN (part 2)

```

 $\{\mathbf{y}, \perp\} \leftarrow \text{vPIN.Dec}(\text{sk}, \llbracket \mathbf{t} \rrbracket_2, \text{cm}, \hat{\pi}, \text{pp}):$ 
35: parse  $\hat{\pi} := (\pi, \text{cm}')$ 
36:  $b \leftarrow \text{CPS.Ver}(\pi, \text{cm}, \mathbf{t}, \text{pp})$ , where  $\text{cm} = (\text{cm}, \text{cm}')$ .
37: if  $b = 1$  then
38:   for  $i = 1$  to  $h$  do
39:      $\mathbf{y}[i] \leftarrow \text{AHE.Dec}(\text{sk}, \llbracket \mathbf{t}[i] \rrbracket_2)$ 
40:   return  $\mathbf{y}$ 
41: else return  $\perp$ 

```

Fig. 8: Our proposed vPIN (part 3)

$\mathcal{F}(\mathbf{W}, \mathbf{C}) \neq \mathbf{t}^*$ and/or $\text{vPIN.Dec}(\text{sk}, \mathbf{t}^*, \text{cm}, \pi^*, \text{pp}) \neq \mathbf{y}$ but $\mathcal{F}'(\mathbf{W}, \mathbf{X}) = \mathbf{y}$, then there are two scenarios:

- Scenario 1: The client accepts the inference proof produced by a dishonest server on the arbitrary model $\hat{\mathbf{W}}$ and/or the arbitrary sample $\hat{\mathbf{C}}$. π^* is verified within the vPIN.Dec algorithm as $\{0, 1\} \leftarrow \text{CPS.Ver}(\pi^*, \text{cm}, \mathbf{t}^*, \text{pp})$. However, the probability of $\text{CPS.Ver}(\pi^*, \text{cm}, \mathbf{t}^*, \text{pp}) = 1$ is negligible in λ , due to the knowledge soundness of the back-end CP-SNARK, which ensures that if a dishonest prover \mathcal{P}^* produces a commitment cm , a proof π^* and inference result \mathbf{t}^* , $\text{CPS.Ver}(\pi^*, \text{cm}, \mathbf{t}^*, \text{pp}) = 1$ iff $\text{cm} = \text{cm}^*$, $\pi = \pi^*$, $\mathbf{W} = \hat{\mathbf{W}}$, and $\mathbf{C} = \hat{\mathbf{C}}$. However, the probability that $\text{cm}^* = \text{cm}$ given $\hat{\mathbf{W}} \neq \mathbf{W}$ is negligible in λ due to the binding property of the commitment scheme. Therefore, it is negligible in λ that $\text{vPIN.Dec}(\text{sk}, \mathbf{t}^*, \text{cm}, \pi^*, \text{pp}) \neq \perp$.

Simulator 1 (Simulation of vPIN for data sample and inference privacy). Let $(\text{sk}, \text{pk}, \text{pp}) \leftarrow \text{vPIN.Setup}(1^\lambda, l)$ for any λ and l . Given $s = n \times m$ as the data sample size, $\mathbf{W} := (\mathbf{F}, \hat{\mathbf{W}}, \hat{\mathbf{b}})$ as the server model, where \mathbf{F} is the convolutional filter and $\hat{\mathbf{W}}, \hat{\mathbf{b}}$ are FC layer's parameters. Let \hat{s} be the stride size and k, \hat{k} be the convolutional filter and pooling window size. Let g, h be the FC layer input and output sizes. Given $n' = ((n - k)/\hat{s}) + 1$ and $m' = ((m - k)/\hat{s}) + 1$, along with $\hat{n} = n' / \hat{k}$ and $\hat{m} = m' / \hat{k}$, the simulator $\hat{\mathcal{S}}$ maintains a copy of the AHE scheme and acts as follows.

- $(\llbracket \mathbf{t} \rrbracket_2, \llbracket \mathbf{C} \rrbracket_2) \leftarrow \hat{\mathcal{S}}(\text{pk}, s, \text{pp})$: $\hat{\mathcal{S}}$ executes $\llbracket c_i \rrbracket_2 \leftarrow \text{AHE.Enc}(\text{pk}, 0)$ for each $i \in [s]$ and invokes $\llbracket \mathbf{A}[i, j] \rrbracket_2 = \sum_{i'=0}^{k-1} \sum_{j'=0}^{k-1} \mathbf{F}[i', j'] \cdot \llbracket \mathbf{C}[i \cdot \hat{s} + i', j \cdot \hat{s} + j'] \rrbracket_2$ for $i \in [0, n']$ and $j \in [0, m']$, where $\llbracket \mathbf{C} \rrbracket_2 = (\llbracket c_1 \rrbracket_2, \dots, \llbracket c_s \rrbracket_2)$. Subsequently, $\hat{\mathcal{S}}$ executes $\llbracket c'_i \rrbracket_2 \leftarrow \text{AHE.Enc}(\text{pk}, 0)$ for each $i \in [s]$ and performs $\llbracket \mathbf{B}[i, j] \rrbracket_2 = \frac{1}{\hat{k}^2} \sum_{i'=0}^{\hat{k}-1} \sum_{j'=0}^{\hat{k}-1} \llbracket \mathbf{C}'[i \cdot \hat{k} + i', j \cdot \hat{k} + j'] \rrbracket_2$, for $i \in [0, n']$ and $j \in [0, m']$ where $\llbracket \mathbf{C}' \rrbracket_2 = (\llbracket c'_1 \rrbracket_2, \dots, \llbracket c'_s \rrbracket_2)$. Next, $\hat{\mathcal{S}}$ invokes $\llbracket \mathbf{d}[i \cdot \hat{m} + j] \rrbracket_2 = \llbracket \mathbf{B}[i, j] \rrbracket_2$ for $i \in [0, \hat{n}]$ and $j \in [0, \hat{m}]$ and computes $\llbracket \mathbf{t}[i] \rrbracket_2 = (\sum_{j=0}^g \hat{\mathbf{W}}^T[i, j] \cdot \llbracket \mathbf{d}[j] \rrbracket_2) + \llbracket \mathbf{b}[i] \rrbracket_2$ for $i \in [0, h]$. Finally, $\hat{\mathcal{S}}$ outputs $\llbracket \mathbf{C} \rrbracket_2$ and $\llbracket \mathbf{t} \rrbracket_2$.

Fig. 9: Simulator of vPIN for data sample and inference privacy.

- Scenario 2: Client accepts \mathbf{t}^* s.t. $\text{vPIN.Dec}(\text{sk}, \mathbf{t}^*, \text{cm}, \pi^*, \text{pp}) = \mathbf{y}^*$ and $\mathbf{y}^* \neq \mathcal{F}'(\mathbf{W}, \mathbf{X})$. We say that this happens with a negligible probability in λ due to the correctness and homomorphic properties of AHE,

which ensure that the (linear) inference computation can be evaluated over the ciphertext domain. vPIN follows the client-aid model, where the server occasionally sends the encrypted evaluation to the client to perform either non-linear operations (e.g., activation function) or truncation. In vPIN, the server always performs homomorphic computation on AHE ciphertext of messages of up to 35 bits and the client always receives the encrypted evaluation results of up to 35 bits. This ensures that the client can always perform the decryption correctly via the discrete log solver.

Data sample and inference privacy. We construct simulator \hat{S} for vPIN (Figure 6, Figure 7, and Figure 8), shown in Figure 9. We create a hybrid game consisting of **Hybrid** $H = (H_1, H_2)$ to prove their indistinguishability as follows

- H_1 : It is the real protocol on the client's encrypted data sample.
- H_2 : It is the simulator \hat{S} in Figure 9.

The server cannot distinguish between H_1 and H_2 due to the IND-CPA security of the back-end AHE scheme where the encrypted data sample C and encrypted inference result t do not reveal any information about the underlying plaintext.